WRC RESEARCH REPORT NO. 140

ADVANCED METHODOLOGY FOR STORM SEWER DESIGN - PHASE II

Harry G. Wenzel, Jr.
Ben Chie Yen
Wilson H. Tang
Department of Civil Engineering
University of Illinois at Urbana-Champaign

FINAL REPORT

Project No. B-098-ILL

This project was partially supported by the U.S. Department of the Interior in accordance with the Water Resources Research Act of 1964, P.L. 88-379
Agreement No. 14-31-0001-6073

UNIVERSITY OF ILLINOIS
WATER RESOURCES CENTER
2535 Hydrosystems Laboratory
Urbana, Illinois 61801

June 1979

ABSTRACT

ADVANCED METHODOLOGY FOR STORM SEWER DESIGN-PHASE II

This report describes further development of computer models for determining the diameter, slope and elevations of each pipe in a storm drainage system in which the layout and manhole locations are specified. The design procedure is based on a least-cost criterion and utilizes discrete differential dynamic programming as the search technique. In this phase of the study a detention storage capability has been added to the model using two approaches. The first approach requires the specification of a maximum allowable outflow and computes the required storage. The second approach determines the storage volume such that the sum of the storage and pipe system costs is a minimum. The procedure for computation of expected damage costs has been changed to reflect the variation of flood damage with flood volume. Also a surface runoff component has been added. This option uses the hydrograph generation portion of the Illinois Urbana Drainage Area Simulator model. Improved cost specification methods as well as flexible pipe elevation constraint capabilities have been added. The new developments are illustrated using two example basins.

Wenzel, Harry G. Jr., Yen, Ben Chie and Tang, Wilson H.
ADVANCED METHODOLOGY FOR STORM SEWER DESIGN-PHASE II
Final Report to the Office of Water Research and Technology, Department of the Interior, Washington, D. C., Research Report No. 140, Water Resources Center, University of Illinois, Urbana, Illinois, June 1979.
KEYWORDS--cost/cost analysis/design-hydraulics/*drainage systems/dynamic programming/effluents-waste water/flood damage/flood routing/hydraulic design/hydraulics/hydrograph routing/mathematical models/methodology/ operations research/*optimization/probability analysis/*risks/safety-factor/ *sewers/sewer systems/*storm drains/storm runoff/systems analysis/uncertainties/*urban drainage/*urban runoff

CONTENTS

LIST OF FIGURES

LIST OF TABLES

NOTATION

A = area

b = coefficient

C_D = expected damage cost

C_F = damage value for a pipe

c = intercept of regression line

D = decision, i.e., drop in elevation in optimization procedure; also, flood damage

d = pipe diameter

E = elevation; also, expected value

F_n = cost function at stage n

$f()$ = function

f_c = final infiltration capacity

f_o = initial infiltration capacity

i = rainfall intensity; also, an index

j = an index

k = an index

m = slope of regression line

m_n = manhole on isonodal line n

N = number of years

n = Manning's roughness factor;

PA = pervious area

Q^* = maximum outflow from detention reservoir

Q_C = sewer capacity

Q_L = peak flow to which a pipe is subjected

Q_p = peak discharge

R = hydraulic radius; also, rainfall depth

r = return; also, interest rate

S = slope; also, state

$\tilde{S}$ = output state

S_o = sewer slope

SIA = supplemental impervious area

s = storage

TR = total rainfall depth

T_r = return period

$T_{m_n,m_{n+1}}$ = connection vector between manholes m_n and m_{n+1}

t_d = duration of hydrograph

t_e = time of concentration

V = storage volume; also, flood volume; also, velocity

z = Q_L/Q_C

Δ = increment

δ = standard deviation of lognormal distribution

λ = mean of lognormal distribution

ϕ = cumulative standard normal probability distribution

CHAPTER 1 INTRODUCTION

This report is a summary of the second phase of a study directed at the development of advanced methodologies for design of sewer systems. This phase was specifically devoted to improvements and additions to the models that were developed in Phase I[12]*.

This chapter contains a brief summary of the models, a statement of the specific objectives of this phase of the study and a summary of the accomplishments.

1.1 Design Philosophy

This study was undertaken with the belief that the existing procedures for sewer system design had remained essentially unchanged for years and did not reflect recent advances in technology. Any engineering design presumably is based on a maximum benefit goal. It is believed that in the case of sewer design the conventional procedures leave much to be desired in terms of explicit steps to maximize benefits. The design methodologies developed in Phase I of this study are a significant step in reaching this goal.

There are three basic components to the new methodology. The first, and perhaps most basic, is the application of optimization techniques. This means that design decisions are made based on a least-cost criteria applied to the entire system. Ideally, all types of costs should be considered including installation, flood damage, operation and maintenance, social, health, and environmental The quantification of all of these costs is a challenge indeed and the work to date has incorporated only installation costs and costs associated with uncertainties and risks.

The second component is a procedure in which the uncertainties or risks associated with the design are recognized, evaluated and their effect on

---

* Superscripts refer to Appendix A: Project Publications

cost included. There are many types of uncertainties which can be considered in addition to the traditional hydrologic risks, including hydraulic, construction, material, costs and damages and uncertainties in the acceptable failure risk level.

The third component is a routing procedure. The traditional rational method of design does not employ hydrograph routing. However, sewer flow is certainly a nonuniform unsteady process and therefore its use is justified. But there are many routing procedures, all of which involve a trade-off between accuracy and time. A number of these were examined in Phase I and it was found that for design purposes a simple hydrograph shifting procedure was sufficient since it is the time shifting of the various hydrograph peaks rather than peak attenuation that is significant.

In addition to these major components any design is subject to some constraints and assumptions. The constraints that are employed in the design methodology are as follows:

(a) Free surface or gravity flow exists under design flow conditions.

(b) Commercially available circular pipes are used in the design with a minimum diameter of 8 in.

(c) The diameter used for design is the smallest commercially available pipe with a capacity equal to or greater than the design flow and which satisfies all constraints.

(d) A minimum cover depth is specified for each pipe.

(e) At a junction the crown elevation of the upstream sewer is equal to or greater than the crown elevations of any of the downstream sewer.

(f) A minimum allowable flow velocity under design flow conditions is

specified to provide self-cleaning capability. This is usually 2 feet per second (fps).

(g) A maximum allowable flow velocity under design flow conditions is specified to minimize excessive scour.

(h) At a junction the diameter of downstream sewers cannot be smaller than any of the upstream sewers.

The assumptions made in the design procedure are:

(a) The sewer system is a downstream converging dendritic network.

(b) Negative sewer slopes are not allowed.

(c) Topographic conditions uniquely determine the direction of flow.

1.2 Summary of Phase I Study

The results of the Phase I study are well documented. The most complete description of all aspects of the methodology is presented in the report by Yen et al.[12] In addition various publications have been written which pertain to one or more aspects. A complete list of project-related publications is presented in Appendix A.

This section presents a brief description of each of the major components of the methodology. For more details the reader is referred to the above-mentioned references.

1.2.1 Optimization Technique

The basic technique employed for optimization is discrete differential dynamic programming (DDDP)[2]. In order to apply this technique to a multi-level branched sewer system the system is represented in terms of lines which pass through all manholes (nodes) which are separated from the system outlet by the same number of pipes (links). These lines are termed isonodal lines (INL)

and they serve to divide the sewer system into stages. Figure 1.1 shows the INL construction for the ASCE Basin system described in Chapter 6. The optimization procedure progresses in the downstream direction stage by stage.

The basic decision variable for each pipe in a stage is the crown elevation at each end of the pipe. Each combination of possible crown elevations (states) has associated with it a cost. The cost is made up of a material cost, installation cost and possibly a cost associated with damage in the event that the sewer capacity is exceeded. The material cost is determined from the pipe size which is related to the capacity and slope using Manning's formula assuming just-full gravity flow.

$$d = [4.66 \frac{n^2 Q^2}{S_o} p]^{3/4} \qquad (1.1)$$

in which d = pipe diameter in ft, n = Manning's roughness; S_o = sewer slope; and Q_p = peak flow in the sewer in cubic feet per second. The slope is computed using the elevations at each end of the pipe. This allows computation of the diameter and hence the cost of the pipe. The crown elevations and the diameter determine the amount of excavation required which is converted to cost. This information can also be used to determine the expected damage cost if desired. It is the objective of the DDDP procedure to minimize the total cost of the system.

The DDDP procedure involves the establishment of an initial set of trial elevations for the entire system called an initial trajectory. A range of possible elevations or corridor on each side of the trajectory is established. Conventional dynamic programming is used within each corridor to determine the least-cost trajectory with the stages, states and objective function as described above. The least-cost trajectory within the corridor is then used as the

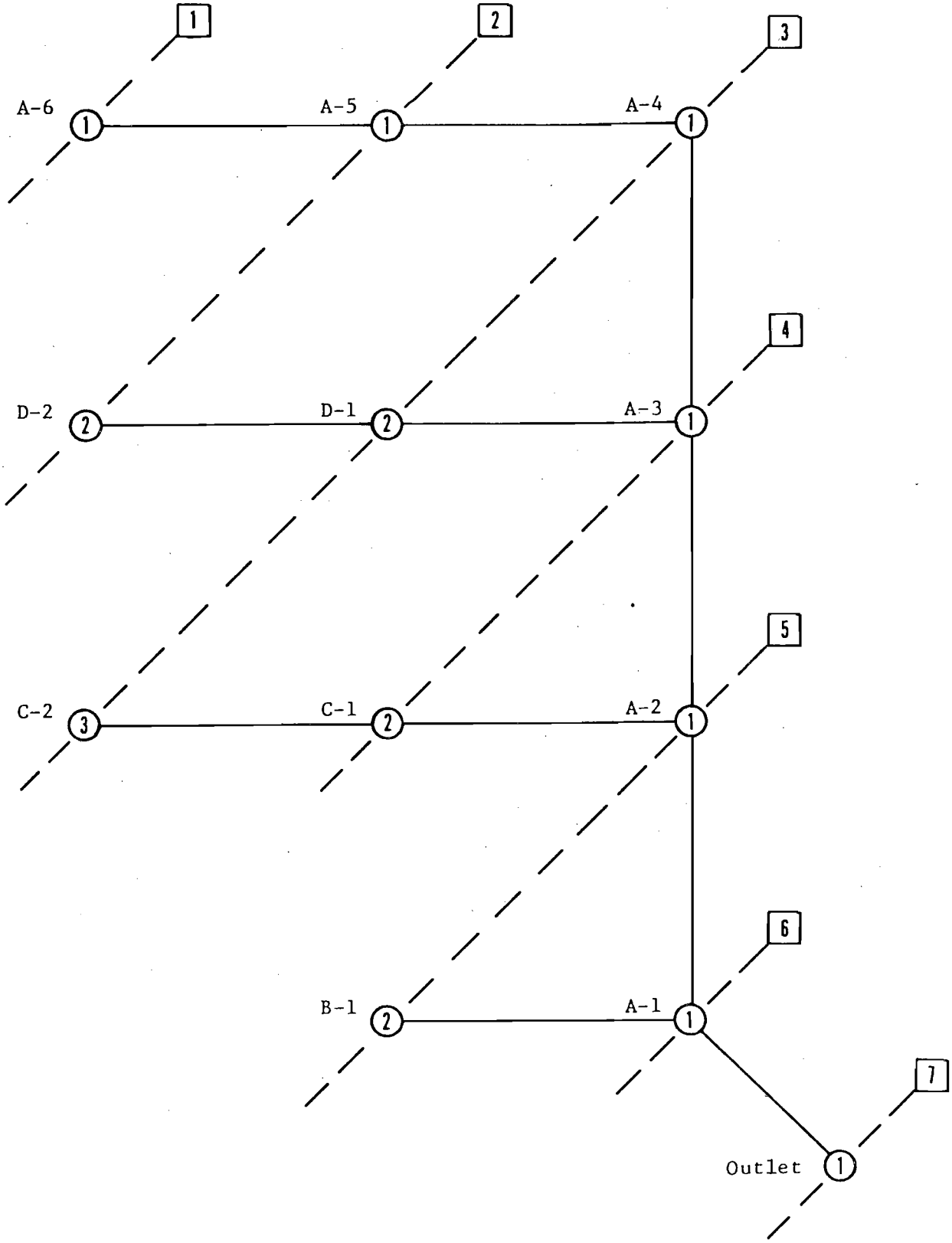

Fig. 1.1 Isonodal Lines for ASCE Basin

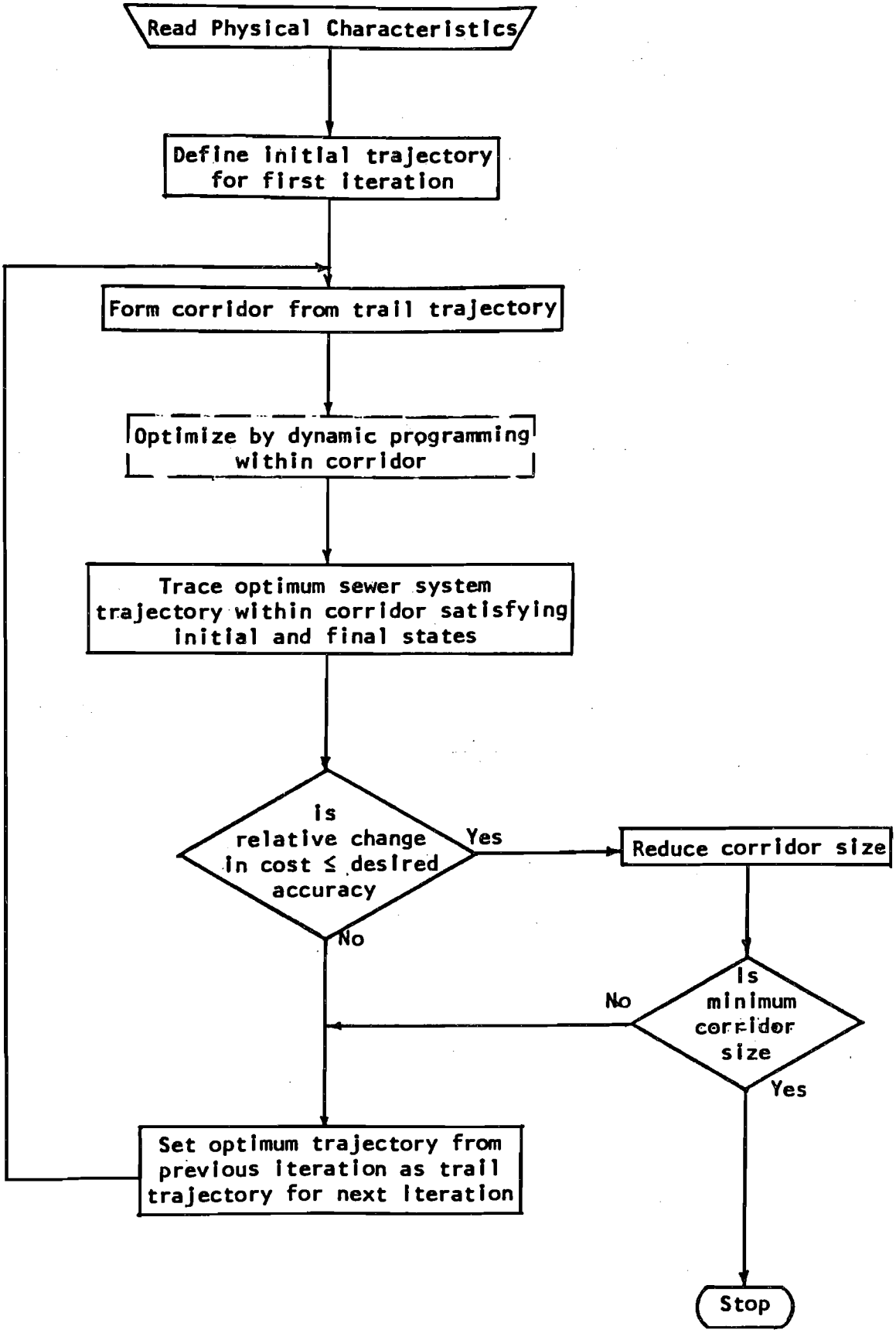

Figure 1.2 DDDP Procedure for System Design

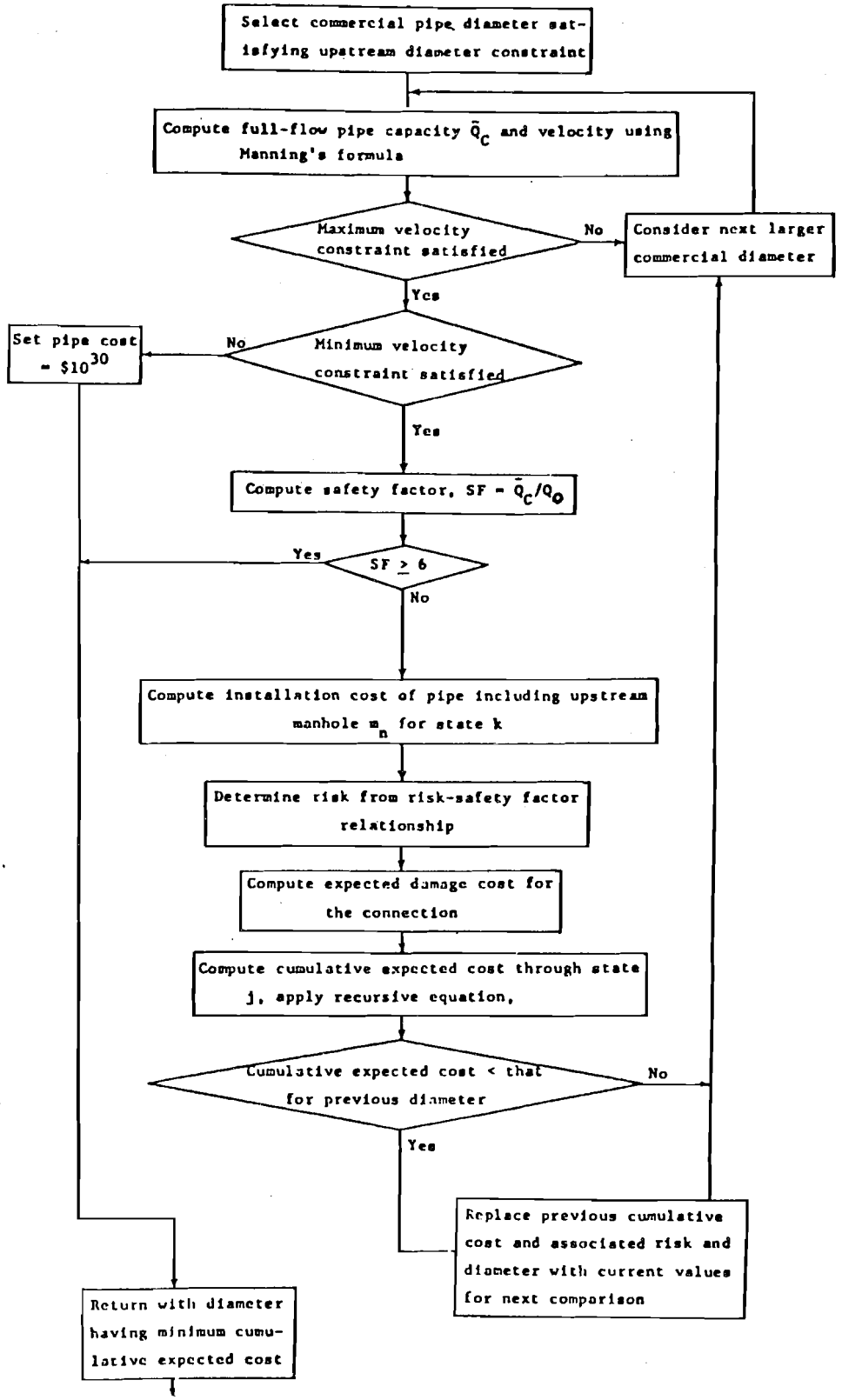

Fig. 1.3. Flow Chart for Sewer Diameter Selection Considering Risks

center of a narrower corridor and the optimization procedure repeated. These iterations are repeated until the reduction in cost for successive iterations falls within a prescribed limit. The major steps in the procedure are shown in the flow chart in Fig. 1.2. For a more detailed description the reader is referred to publications 4, 9 and 12 in Appendix A.

1.2.2 Risk Considerations

The purpose of including risk analysis in the design is to quantitatively estimate the costs associated with a number of the various uncertainties in the capacity of a given pipe, Q_C, or the peak flow, Q_L, to which the pipe is subjected. The risk of failure can be defined as the probability of the event $Q_L > Q_C$.

$$\text{Risk} = P(Q_L > Q_C) = P[\ln(Q_C/Q_L) < 0] \tag{1.2}$$

To evaluate the cost associated with the risk an "assessed damage value" is used. This is defined as the damage value, C_F, associated with a given pipe in the event that $Q_L > Q_C$. The expected damage cost, C_D, is then given by

$$C_D = C_F \ [P(Q_L > Q_C)] \tag{1.3}$$

This is a first attempt at incorporating damage costs into the model and this report describes an improved approach.

The evaluation of the risk is facilitated by the introduction of the safety factor, SF, which is defined as the ratio of the capacity of a pipe, Q_C, as determined by a hydraulic formula such as Eq. 1.1, to the peak flow that the sewer is estimated to be required to carry, Q_p, as determined by some hydrologic analysis. The relationship between risk and safety factor can be

established by analyzing the various factors which contribute to the overall risk. This procedure is described in references 4, 7 and 12 in Appendix A. This relationship is then used within the optimization procedure to evaluate the total cost associated with each pipe. Figure 1.3 shows a flow chart which describes the detailed procedure for a specific pipe within the overall optimization procedure described in Fig. 1.2.

1.2.3 Routing Procedures

A number of flow routing procedures were investigated in the Phase I study. It was desired to adopt a method which reflected the important effects of unsteady flow as far as design is concerned, while requiring a minimum amount of computer time to execute.

Three routing methods were programmed: a nonlinear kinematic wave method, a modified Muskingum method and a time-lag method. It was determined that the important feature of the routing process was the relative timing of the in-system hydrographs and the inlet hydrographs at the manholes. The attenuation of the peaks is important only for very large systems.

It was found that the time lag routing procedure was adequate for design purposes and is the method recommended for future use in the model. It involves simply the shifting of the inflow hydrograph by a time increment t_f which is the flow time through the pipe estimated by computing the full flow velocity at peak inflow. The inlet hydrograph is added to the routed hydrograph for a pipe. After routing a linear interpolation scheme is used to determine the outflow hydrograph ordinates at the prescribed time increments used in the overall time scale.
used in the overall time scale.

1.2.4 Models Developed Under Phase I

The basic model components were formulated in various combinations as shown in Table 1.1. The DDDP technique is common to all with various types of routing procedures incorporated both with and without risk.

Table 1.1 Least-Cost Sewer Design Models-Phase I

Model Designation	Routing Procedure	Risk Analysis Incorporated
A	None	No
B-1	Time Lag	No
B-2	Kinematic Wave	No
B-3	Modified Muskingum	No
C	None	Yes
D	Time Lag	Yes

The model designation shown in Table 1.1 was utilized in the Phase I completion report. Subsequently Models B-1 and D have been refined and renamed as Models ILSD-1 and ILSD-2, respectively, for presentation in workshops and for practical applications.

1.3 Objectives of Phase II Study

The general objective of this study is to refine and further develop the methodology and techniques developed in Phase I.

Specific objectives are as follows:

(a) Develop a detention storage component and incorporate it in the models.

(b) Refine the risk analysis component with specific emphasis on improvement in flood damage determination.

(c) Incorporate a surface hydrology model which will determine sewer inlet hydrographs.

(d) Incorporate a method to facilitate design of multiple branch systems.

(e) Incorporate minor refinements and improvements that have been suggested through experience subsequent to Phase I.

1.4 Summary of Phase II Accomplishments

There have been three major improvements in the methodology as a result of this study.

1. The capability of utilizing detention storage in the design has been added to the model. Two approaches were developed. The first permits the specification of a maximum allowable flow downstream of the detention reservoir. The hydraulic effects of this are included in the design procedure but the storage costs are not included in the costs that are minimized. The second approach requires the specification of a maximum allowable storage volume and incorporates the storage cost together with the other costs and the total is

minimized. The storage volume corresponding to a minimum total cost is computed. Both approaches are discussed in Chapter 2.

2. The method for computing expected damages resulting from risk considerations has been improved. The procedure involves the use of depth-damage, depth-flood volume and flood peak-risk relationships. This method recognizes the variation of flood damage with the magnitude of the flood volume. The method is described in Chapter 3.

3. A surface runoff component option has been added. This relieves the user from independently determining the inlet hydrographs. The option requires rainfall and sub-catchment data and computes runoff hydrographs using the time-area method. The option uses the runoff computation portion of another model, the Illinois Urban Drainage Area Simulator (ILLUDAS) developed at the Illinois State Water Survey. The details are presented in Chapter 4.

In addition a number of more minor improvements have been added including cost data specification, negative slope checks and optional elevation and and pipe size constraints. These are discussed in Chapter 5.

CHAPTER 2. DETENTION STORAGE

Detention storage is becoming an increasingly important design tool in urban drainage. However design procedures are far from being standardized. This makes the incorporation of detention storage into the model a difficult task and the effort reported here should be regarded as an initial approach subject to further improvement.

Two approaches to including detention storage in the design model have been taken. The first approach accounts for the reduction in peak flow downstream using a prescribed maximum outflow from a reservoir. However, the cost of the reservoir itself is not included in the total cost of that stage in the design and hence the reservoir cost is excluded from the optimization procedure. In the second approach the reservoir size (storage capacity) is another decision variable with its cost included as part of the total system cost which is minimized. In both approaches the location of the reservoir(s) is independently determined. These approaches are described in this chapter.

2.1 Detention Storage: Non-Optimization Approach

In this approach the costs of the detention reservoirs are computed separately and not included in the costs considered for optimization. The location of the detention reservoir is predetermined independently and it is assumed to be located at the upstream end of a designated reach with a sewer pipe connecting it to the downstream manhole. The inflow hydrograph to the reservoir is assumed to be the outflow hydrograph from the manhole. The pipe leading from the reservoir outlet is designed using the peak discharge of the reservoir outflow hydrograph.

The design criterion for the reservoir is the maximum allowable outflow which is specified by the user. Figure 2.1 shows the assumed operation of

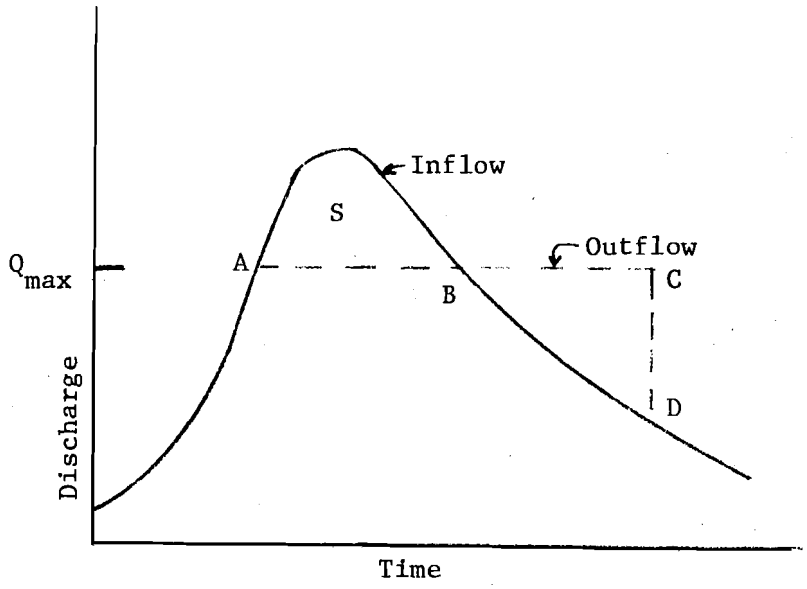

Fig. 2.1 Detention Reservoir Operation for Non-Optimization Approach

the reservoir. When the inflow hydrograph reaches the maximum permitted outflow Q_{max} (point A in Fig. 2.1) the outflow hydrograph is assumed to remain constant and detention storage volume S is accumulated at point B. The required volume S is simply the area between the inflow hydrograph and the outflow hydrograph AB. The outflow hydrograph remains at Q_{max} until the storage is depleted (point C) at which time the outflow is assumed to drop down to the inflow hydrograph (point D).

It is recognized that detention reservoirs do not produce the flat outflow hydrograph shown in Fig. 2.1. The specific type of outlet controls will dictate the outflow hydrograph shape. However the assumed operation represents an initial approach. It does retain the desired downstream peak flow limitation and it is unlikely that the actual outlet hydrograph shape will have a significant effect on the design of the downstream system.

The required detention storage capacity S is computed and the associated cost is calculated using a specified unit storage cost. This cost is simply added to the other system costs at the stage in which the reservoir is located. Thus detention storage is not a decision valuable in the optimization procedure and its cost is independent of the design. It is carried along for accounting purposes only. Chapter 6 shows examples of this approach.

2.2 Detention Storage: Optimization Approach

In this approach the storage volume is a decision variable in the cost optimization rather than a parameter determined by specifying a maximum allowable discharge from the reservoir. Thus for any stage there are in general two variables involved: pipe elevation and detention storage volume. This represents a basic change in the DDDP procedure and significantly increases the execution time and computer storage requirements for the program.

The location of each reservoir is predetermined and specified as in the non-optimization approach. Each reservoir is again assumed to be located just below the upstream manhole. Instead of a specified maximum outflow from the reservoir, a series of trial storage volumes is evaluated at each stage where a reservoir is located. Figure 2.2 shows the reservoir operation for a trial storage volume. The trial volumes are initially determined by dividing the total specified maximum permissible storage volume into a series of 4 equal increments.

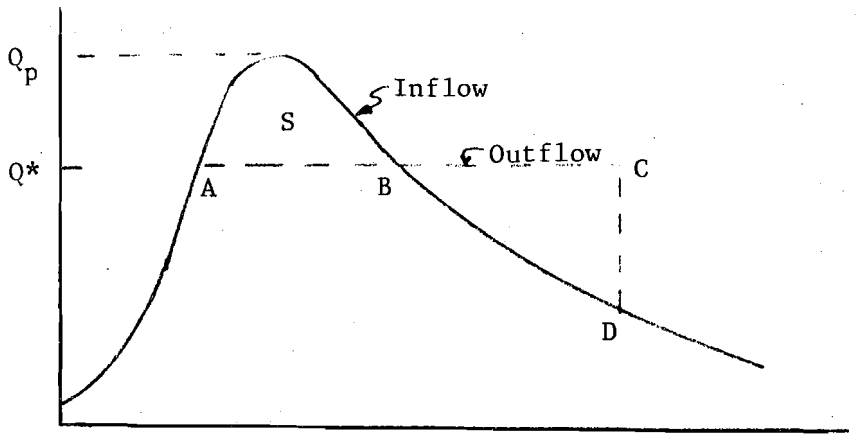

Fig. 2.2 Detention Reservoir Operation for Storage Optimization Approach

Let S represent a trial storage volume. A maximum outflow Q* is computed such that the area between the inflow hydrograph and AB in Fig. 2.2 is equal to the trial storage S. As before this flow rate continues to point C when the storage is depleted at which time the outflow drops down to the inflow hydrograph at point D. It is possible that one or more of the trial storage volumes will be greater than the entire inflow volume of the inflow hydrograph. In that case Q* is arbitrarily set at $Q_p/5$ since it is assumed that the reservoir will not retain all the flow regardless of its storage capacity. There is an exception to this step which is explained in Section 2.2.2.

2.2.1 General Optimization Procedure Including Detention Storage

In the Full Optimization Detention Storage Model not only the pipe diameters and elevations but also the detention storage volumes are optimized. The algorithm for the model has been formulated so that for each possible pipe elevation lattice point on the upstream end of the pipe, there are five trial storage volumes. Although any odd number of trial storage volumes could be used, five values were chosen as a balance between level of refinement and storage and computer time requirements. These storage volumes are analogous to the lattice points used for optimization of the pipe elevations. This does not mean that a storage volume must be specified for each and every pipe. The model has been designed so that all or none of the pipes in the network can have detention storage specified for them. The optimization proceeds by considering various possible pipe elevation/storage volume combinations and determining the cheapest. However, since only some of the pipes will have detention storage specified there are two possibilities for the allowable combinations of storage volumes and pipe elevations. These possibilities are described below.

a) No detention storage specified for the stage (pipe) under consideration.

In this case only one storage level (volume) is specified for each downstream pipe elevation. In face, this storage level is not used and is

merely an index to help identify the pipe elevation lattice point. No routing is performed through this dummy volume. This storage level index in this case is set to 1, i.e., the first storage index encountered in the elevation level/ storage volume combinations. This is shown in Fig. 2.3.

b) Detention storage has been specified at the stage (pipe) under consideration.

In this case all possible combinations of storage volume level and pipe elevation at the upstream end of the pipe must be considered. Routing must be performed through each of the storage volumes. The details of this procedure are discussed in the next sections.

2.2.2 Optimization Algorithm Description

The overall optimization procedure, DDDP, involves a successive series of iterative dynamic programming applications. The state space is redefined after each iteration. In the case of detention storage there are two sets of states at each stage: pipe elevations and storage levels. Figure 2.4 shows a typical stage. For each upstream pipe elevation there are trial storage volumes and correspondingly 5 reservoir outflow hydrographs which can be used to design the pipe. Each combination of pipe elevation and storage volume must be examined.

The dynamic programming procedure can be represented mathematically using the recursive equation for each pipe. Let S_{m_n}, m_{n+1} represent the input state (out of crown elevations) at the upstream end of a pipe from manhole m_n to m_{n+1} where n represents the isonodal line number and m is the manhole number. The two decisions involved are the drop in crown elevation from the upstream to the downstream end of the pipe, $D_{m_n, m_{n+1}}$ and the detention storage volume used at that stage, V_{m_n}. The return (cost) at stage n for the pipe is represented by $r_{m_n, m_{n+1}}$. The recursive equation for each pipe at stage n is

$$F_n(\tilde{S}_{m_n, m_{n+1}}) = \underset{D, V}{\text{Min}}[r_{m_n, m_{n+1}}, (S_{m_n, m_{n+1}}, D_{m_n, m_{n+1}}, V_{m_n}) + F_{n-1}(\tilde{S}_{m_{n-1}, m_n})] \quad (2.1)$$

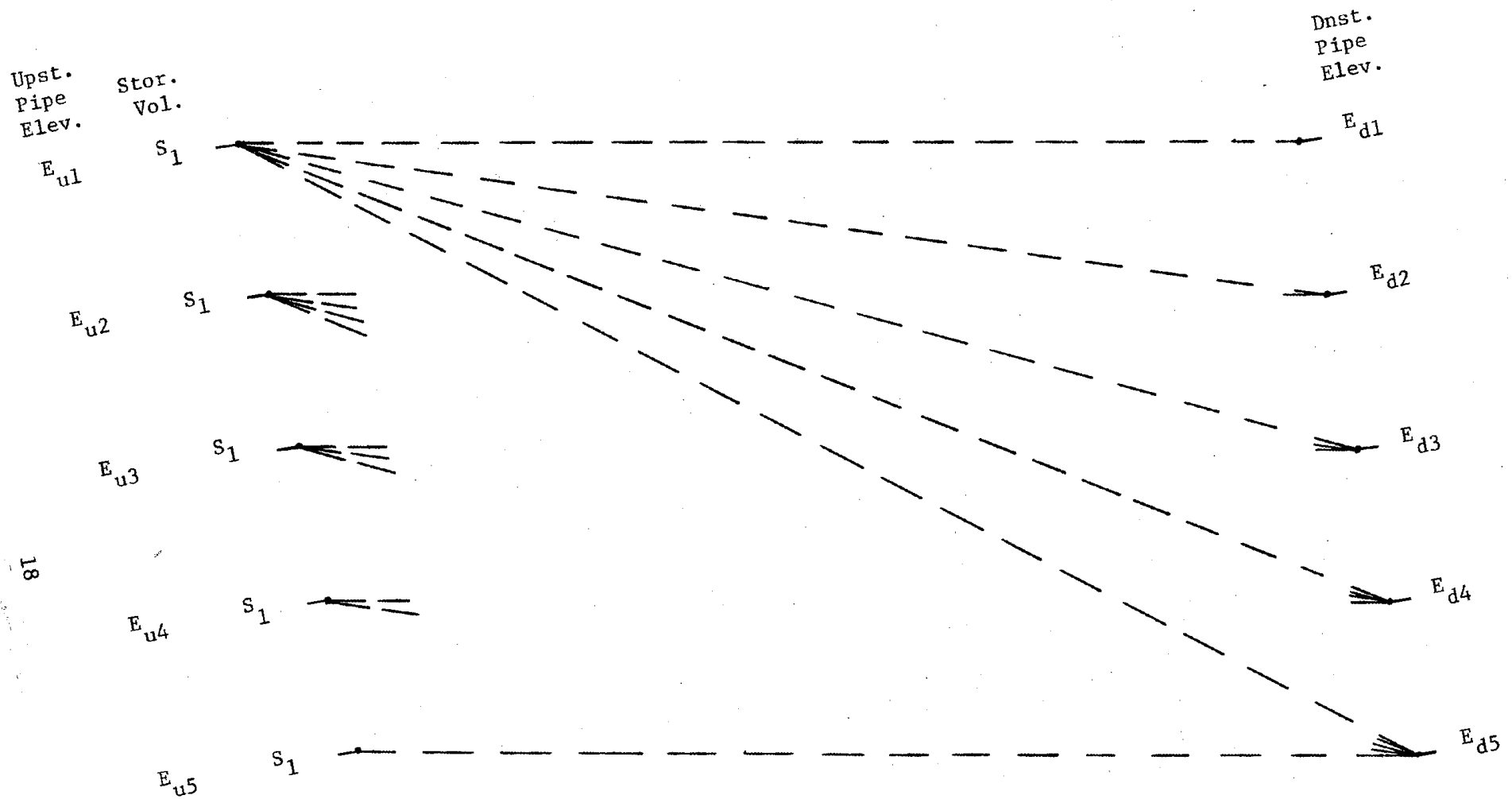

Fig. 2.3 Trial Connections Without Detention Storage

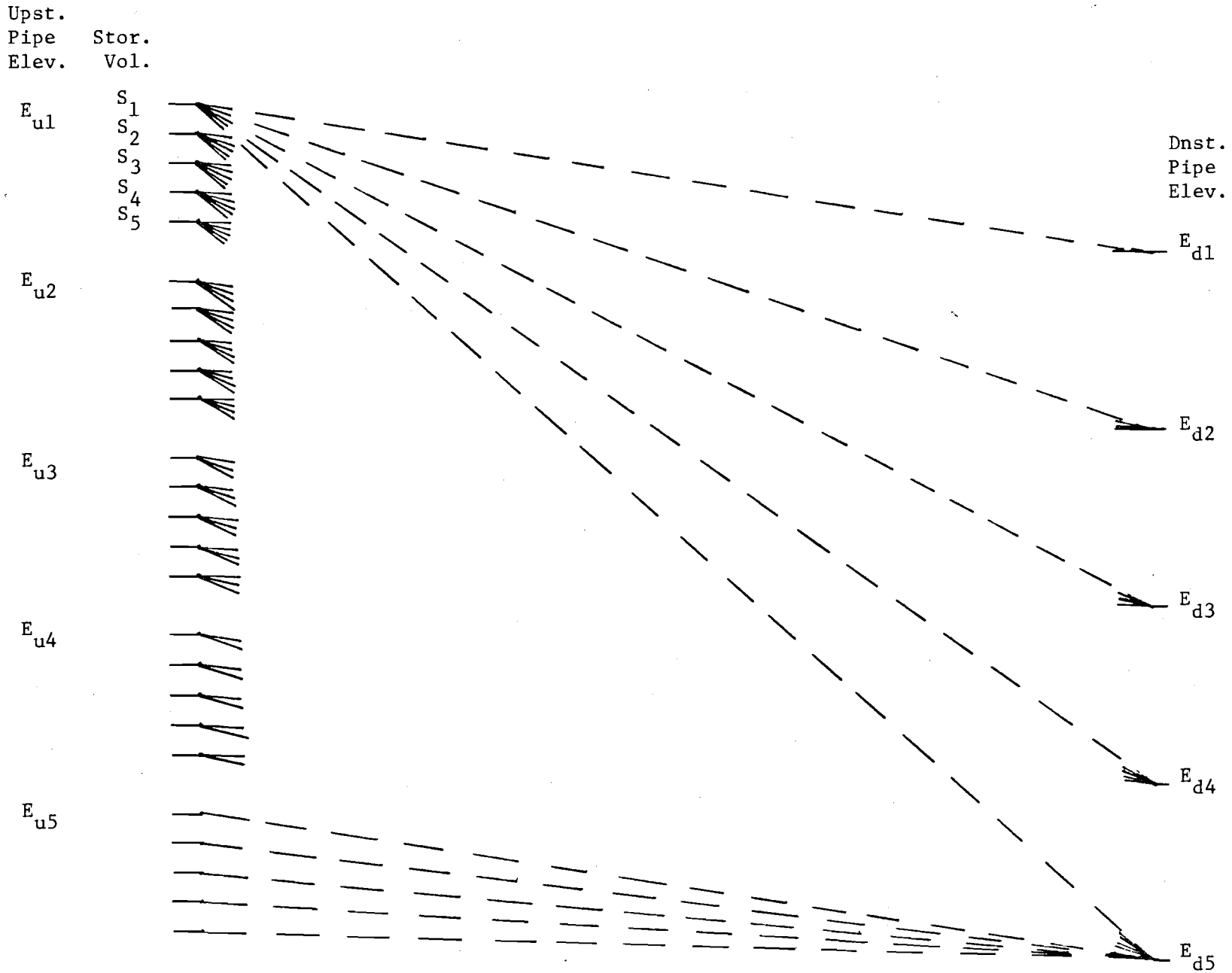

Fig. 2.4 Trial Connections With Detention Storage

where $F_n(\tilde{S}_{m_n}, _{m_{n+1}})$ represents the minimum cost of the system from its upstream and through manholes m_n and m_{n+1}. This procedure is repeated for all pipes connecting to manhole m_{n+1} from isonodal line n. The recursive equation considering all connections to manhole m_{n+1} is

$$F_n(\tilde{S}_n) = \underset{T_{m_n}, m_{n+1}}{\text{Min}} \Sigma F_n(\tilde{S}_{m_n}, _{m_{n+1}}) \qquad (2.2)$$

where $T_{m_n}, _{m_{n+1}}$ is a vector of connections which identifies whether a pipe connects manholes m_n and m_{n+1}.

The case where the trial storage volume exceeds the inflow volume bears further discussion. First it again should be pointed out that in this case the outflow hydrograph from each trial reservoir is assumed the same, with a maximum flow of $Q_p/5$. Thus, for the same combination of upstream and downstream elevations the same pipe diameter will be chosen. However, if more than one trial storage volume exceeds the inflow volume the smallest trial storage volume for that stage will be chosen since it has the least associated cost.

Again for the case where the trial storage volume exceeds the inflow volume, it is possible that $Q_p/5$ is greater than Q^* (see Fig. 2.2) for the previously considered least-cost combination of pipe elevation and storage volume. In that event the minimum of the two values is taken as the Q^* value for the current trial storage volume under consideration. This step helps to insure that more of the excess storage capacity is utilized.

Figure 2.5 is a flow chart which shows the steps involved in one iteration of the DDDP procedure. The establishment of the trial storage levels or state space for storage is discussed below.

The traceback procedure at the end of each iteration establishes a least-cost path in terms of pipe elevations and storage levels. This solution

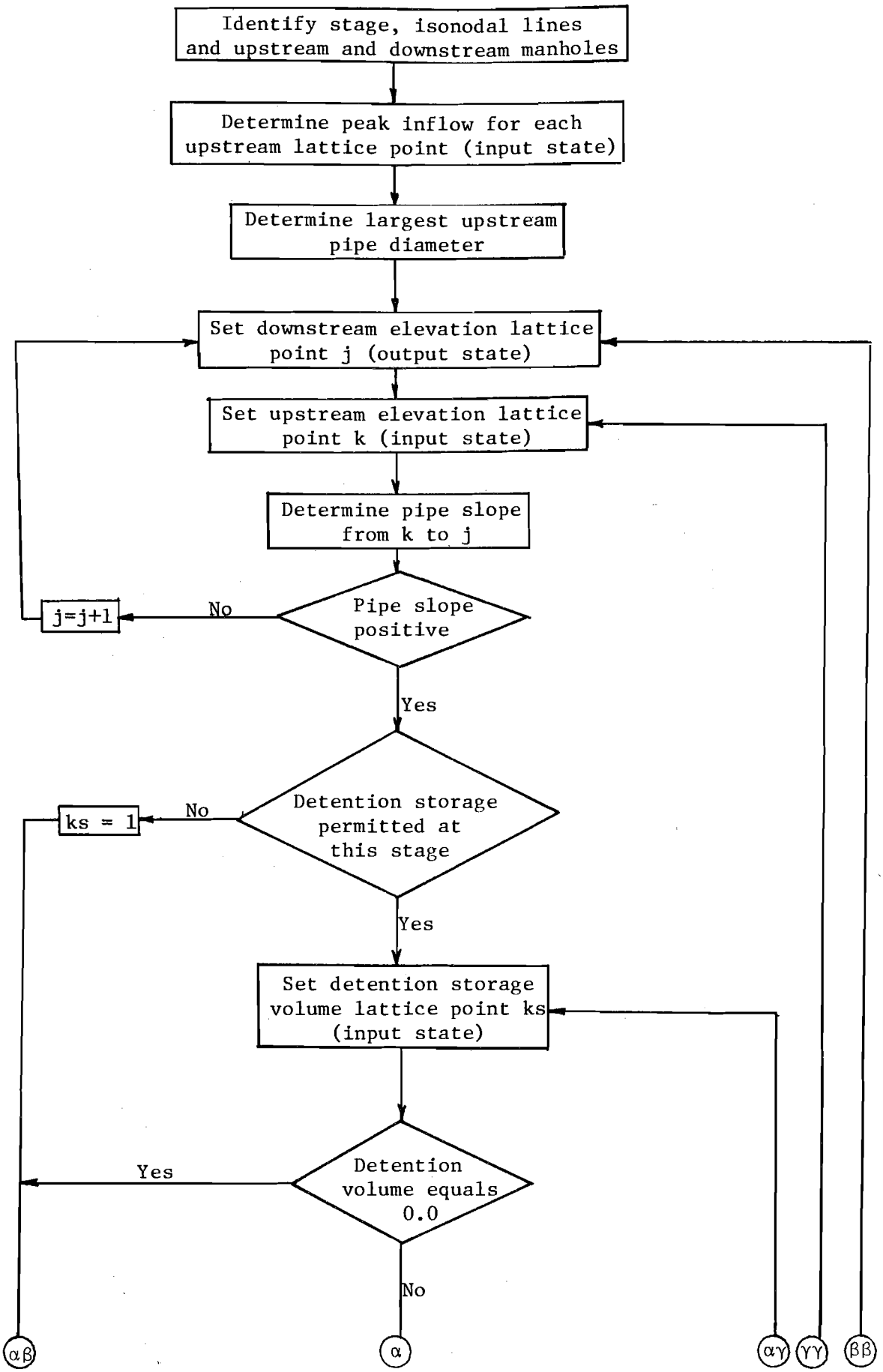

Fig. 2.5 DDDP Procedure Including Detention Storage

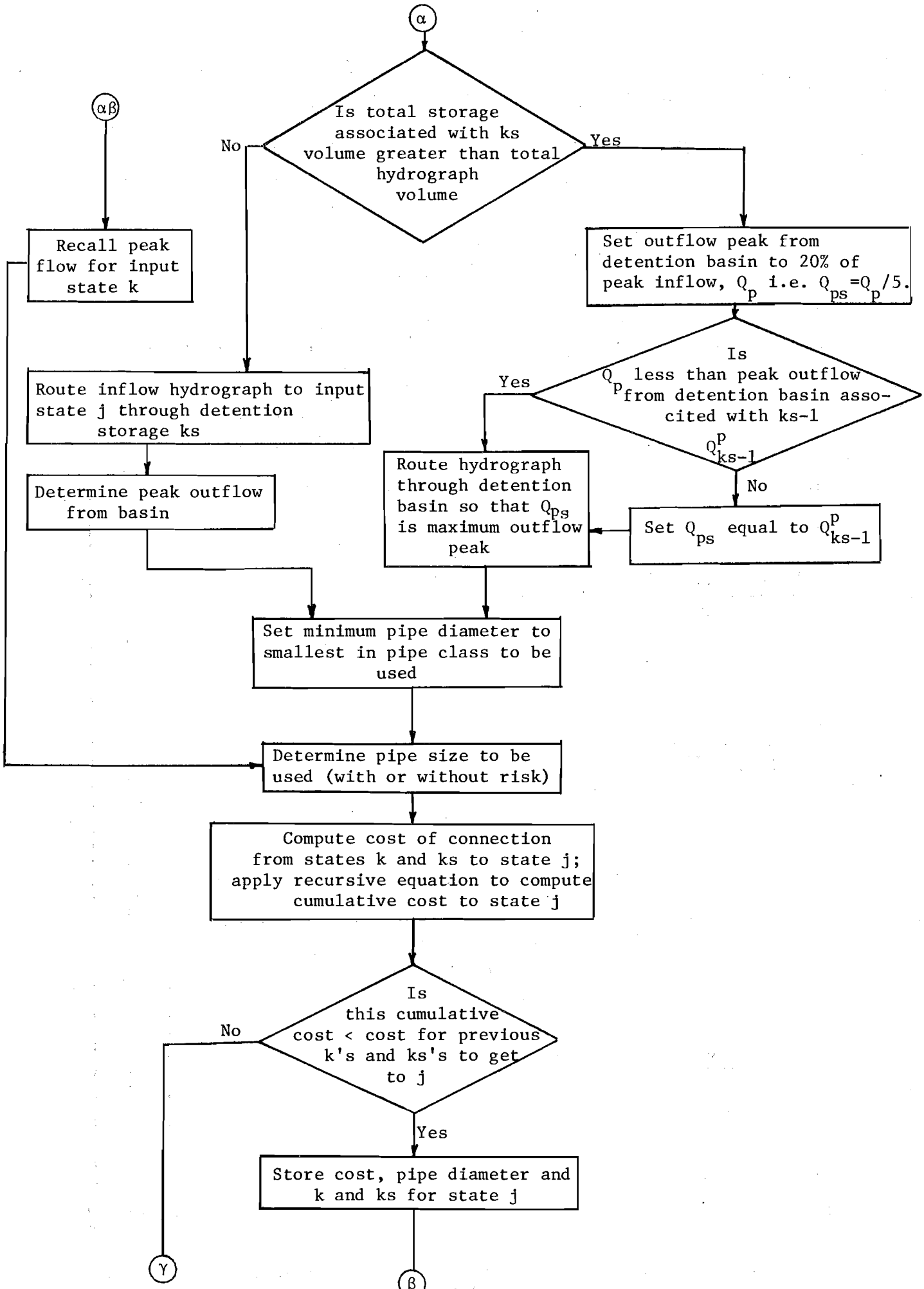
α
αβ
Is total storage associated with ks volume greater than total hydrograph volume
No
Yes
Recall peak flow for input state k
Set outflow peak from detention basin to 20% of peak inflow, Q_p i.e. $Q_{ps}=Q_p/5$.
Is Q_p less than peak outflow from detention basin associated with ks-1 Q^p_{ks-1}
Yes
No
Route inflow hydrograph to input state j through detention storage ks
Route hydrograph through detention basin so that Q_{ps} is maximum outflow peak
Set Q_{ps} equal to Q^p_{ks-1}
Determine peak outflow from basin
Set minimum pipe diameter to smallest in pipe class to be used
Determine pipe size to be used (with or without risk)
Compute cost of connection from states k and ks to state j; apply recursive equation to compute cumulative cost to state j
Is this cumulative cost < cost for previous k's and ks's to get to j
No
Yes
Store cost, pipe diameter and k and ks for state j
γ
β

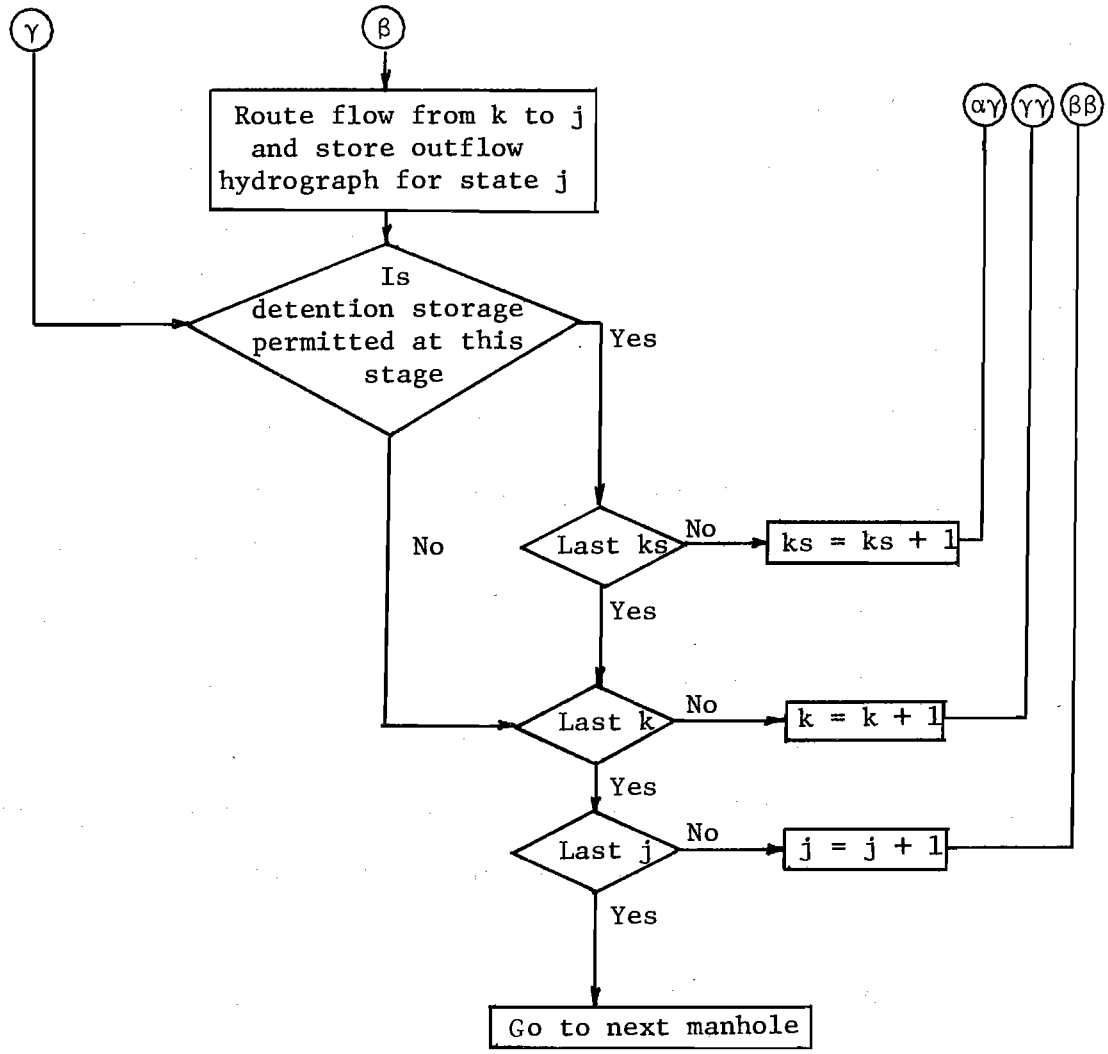
γ
β
Route flow from k to j and store outflow hydrograph for state j
αγ
γγ
ββ
Is detention storage permitted at this stage
Yes
No
Last ks
No
ks = ks + 1
Yes
Last k
No
k = k + 1
Yes
Last j
No
j = j + 1
Yes
Go to next manhole

or trajectory is used as the midpoint of a new set of trial elevations and storage volumes (corridor). The 5 storage volumes are generally determined by halving the storage increment from the previous iteration and then adding and subtracting respectively one and two increments from the least-cost volume from the previous iteration. There are two exceptions to this general procedure: either (a) one of the new trial volumes is greater than the specified maximum storage or (b) one of the new trial volumes is less than zero.

Case (a) - This case is possible either during the fifth iteration when all of the state spaces increments are doubled in order to help insure that local minima are avoided or if the least-cost volume from the previous iteration was the maximum specified storage. In this case the storage state space is determined by setting the maximum trial storage volume equal to the specified maximum storage and incrementing downward 4 equal increments to establish the remaining trial levels.

Case (b) - This case could also be possible either in the fifth iteration as described above or if the least-cost volume from the previous iteration was zero. Here, the storage state space is established by setting the lowest trial storage at zero and incrementing upwards 4 increments to establish the remaining trial volumes.

Chapter 3. RISK-DAMAGE COSTS

3.1 Background

Since the design flood of a storm sewer is only one of the many floods that may occur during its expected service life, there is a probability that floods exceeding the design magnitude may also occur during the expected service life, causing damages to the sewer system and the areas it drains. The assessment of the expected flood damage cost is a complicated and difficult task. The major factors that should be considered include:

(a) the magnitude (depth and volume) of the flood and its occurrence probability;

(b) the capacity of the sewer;

(c) the temporal and spatial distributions of the flood water which in turn depend on the physical characteristics of the drainage area and the rainfall;

(d) the values of the facilities in the drainage area, and the losses that the flood may impose on these facilities; and

(e) the discount rate and expected service period of the sewer.

With the present knowledge and computer capability, it is not possible to account for precisely all the above factors. Some assumptions and simplifications are necessary to permit inclusion of the expected damage cost in the optimization for a least-cost system design. In the previous Phase I project, the damage cost in the event of insufficient sewer capacity was assumed to be a constant value regardless of the magnitude of the flood. The expected damage cost is computed as the probability of a flood exceeding the expected sewer capacity multiplied by this constant damage cost. This

simplified model was adopted partly as a first step to demonstrate how the damage cost can be included in the optimization procedure. In the present project a substantial improvement is made by considering the damage cost as a function of the volume of the flood. The following sections serve as an example to illustrate how the improved method can be used for sewer design.

3.2. Flood Volume - Damage Cost Relationship

The design of a storm sewer generally uses a peak rate of flow as the major design parameter. Figure 3.1 shows an inflow hydrograph with a peak inflow Q_L. Let Q_C be the flow capacity of the sewer pipe. When Q_L exceeds Q_C, the capacity of the pipe is inadequate to handle the inflow and the excess water will cause flooding. The volume of water indicated by the shaded areas in Fig. 3.1 thus represents the total flood volume. For given values of Q_C, Q_L, and shape of hydrograph, the corresponding volume of flood water can be determined.

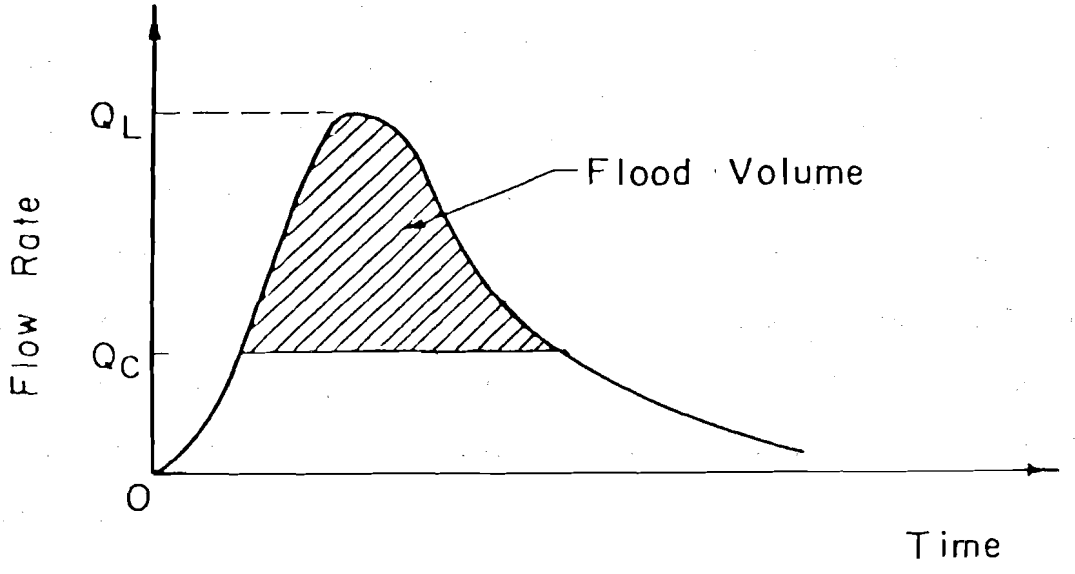

Figure 3.1. Inflow hydrograph

Flooding can result in damages to properties in the vicinity of the sewer pipe. The relationship for volume of flooding and total damage cost can be established from the relationship between the volume and depth of the floods and the relationship between the flood depth and damage cost as shown in Fig. 3.2 (Tang et al. [13]). The resulting relationship for an example given in Tang et al.[13] is shown in Fig. 3.3 for which the relationship between the flood volume V and damage cost, $D(Q_L,Q_C)$, whenever flooding occurs is approximately linear, i.e.,

$$D(Q_L,Q_C) = aV + b \tag{3.1}$$

If the inflow hydrograph (Fig. 3.1) is approximated by a triangle with a base equal to the duration t_b and peak equal to Q_L, the flood volume is the area above the horizontal line Q_C, i.e.,

$$V = \frac{1}{2}\frac{t_b}{Q_L}(Q_L-Q_C)^2 \tag{3.2}$$

Consequently, the damage cost is

$$D(Q_L,Q_C) = \frac{at_b}{2Q_L}(Q_L-Q_C)^2 + b \tag{3.3}$$

3.3. Expected Annual Flood Damage

As discussed in Chapter 5 of Yen et al.[12] both Q_L and Q_C are random variables subject to risks and uncertainties. For statistically independent Q_L and Q_C the expected annual flood damage may be expressed mathematically as

$$D_A = \int_0^\infty \int_0^\infty D(Q_L,Q_C)\, f(Q_C)\, f(Q_L)\, dQ_C\, dQ_L \tag{3.4}$$

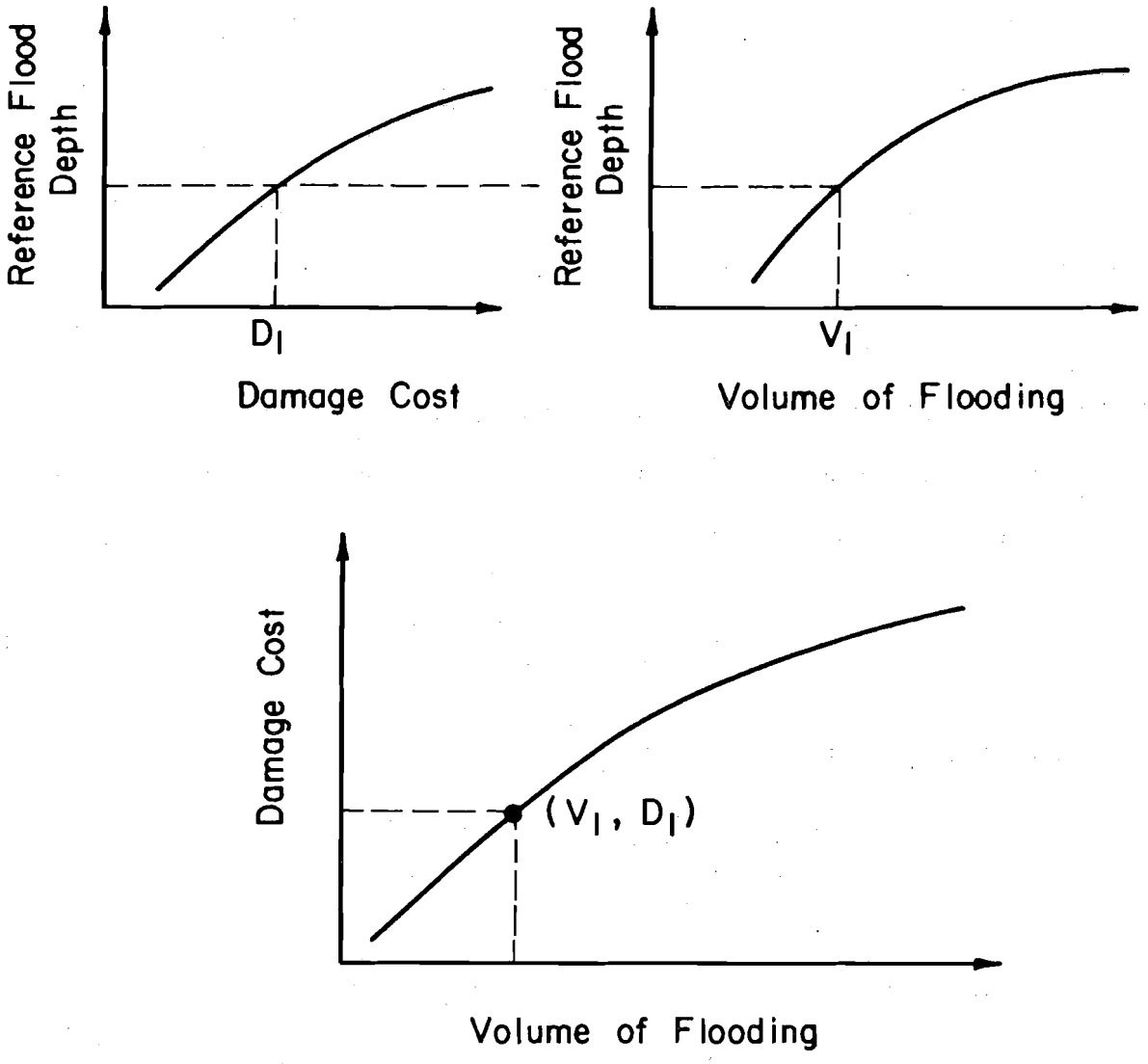

Figure 3.2. Damage Cost - Flood Volume Relationship

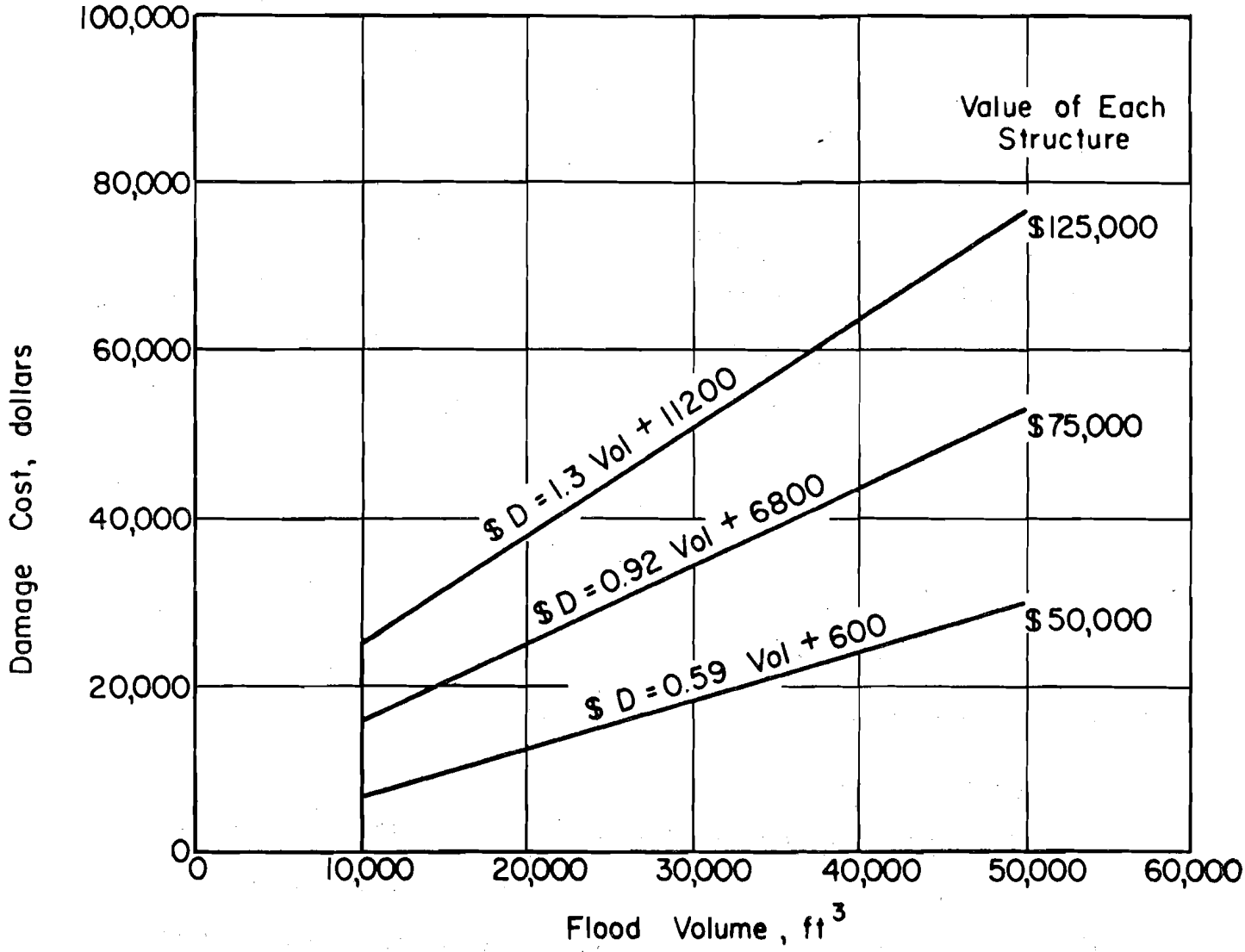

Figure 3.3 Hypothetical Flood Volume - Damage Cost Curve for a Drainage Basin

where $D(Q_L, Q_C)$ = flood damage for given known values of Q_L and Q_C; and $f(Q_L)$ and $f(Q_C)$ are respectively the probability density functions of Q_L and Q_C. Assuming lognormal distributions for Q_L and Q_C (Tang et al.[4]).

$$f(Q_L) = \frac{1}{\sqrt{2\pi}\, Q_L\, \delta_{QL}} \exp\left[-\frac{1}{2}\left(\frac{\ell n\, Q_L - \lambda_{QL}}{\delta_{QL}}\right)^2\right] \qquad (3.5)$$

$$f(Q_C) = \frac{1}{\sqrt{2\pi}\, Q_C\, \delta_{QC}} \exp\left[-\frac{1}{2}\left(\frac{\ell n\, Q_C - \lambda_{QC}}{\delta_{QC}}\right)^2\right] \tag{3.6}$$

in which λ_{QL}, λ_{QC} and δ_{QL}, δ_{QC} are respectively, the means and standard deviations of the transformed random variables $\ell n Q_L$ and $\ell n Q_C$. According to Ang and Tang*, for coefficients of variation Ω for Q_L and Q_C less than 0.3, $\delta_{QL} \simeq \Omega_{QL}$ and $\delta_{QC} \simeq \Omega_{QC}$. Moreover,

$$\lambda_{QL} = \ell n\, \bar{Q}_L - \frac{1}{2}\, \delta_{QL}^2 \tag{3.7}$$

and

$$\lambda_{QC} = \ell n\, \bar{Q}_C - \frac{1}{2}\, \delta_{QC}^2 \tag{3.8}$$

where the bar represents mean value of the parameter.

3.4. Estimation by Double Integration

The expected annual damage cost expressed in Eq. 3.4 involves double integration and its evaluation may be accomplished in two stages. First, for a given Q_L, the expected flood damage, $D(Q_L)$, can be computed by integrating the damage function, $D(Q_L,Q_C)$, over possible values of Q_C,

$$D(Q_L) = \int_0^\infty D(Q_L,Q_C)\, f(Q_C)\, dQ_C \tag{3.9}$$

The integration limits of 0 to ∞ can be simplified by integrating within the limits of $Q_C = 0$ to Q_L because when $Q_C \geq Q_L$ there is no flooding (see Fig. 3.1) and consequently $D(Q_L, Q_C) = 0$.

---

* Ang, A.H.S. and W. H. Tang, Probability Concepts in Engineering Planning and Design, Vol. I: Basic Principles, John Wiley and Sons, 1975.

To account for the randomness of the inflow, values of Q_L corresponding to several equivalent return periods are considered. For each return period T_r, the probability of exceedance is $1/T_r$. Hence the corresponding value of Q_L is associated with the $(1-1/T_r)$ percentile value of the lognormally distributed inflow, which may be computed from

$$Q_L = \exp\left[\lambda_{QL} + \delta_{QL}\, \phi^{-1}\left(1 - \frac{1}{T_r}\right)\right] \tag{3.10}$$

where $\phi^{-1}(\,)$ is the inverse of the cumulative standard normal distribution defined as

$$\phi(z) = \int_{-\infty}^{z} \frac{1}{\sqrt{2\pi}} \exp\left(-\frac{1}{2} x^2\right)\, dx \tag{3.11}$$

For each return period T_r, $D(Q_L)$ is computed using Eq. 3.9 for a specified pipe diameter and slope. The resulting value of $D(Q_L)$ and the respective probability of exceedance in any given year $(1/T_r)$ can be plotted to establish a damage-frequency curve as shown in Fig. 3.4a for a given pipe diameter and slope. The area under this damage-frequency curve is the average annual expected damage which can be expressed as

$$D_A = \int_0^{\infty} D(Q_L)\; f(Q_L)\; dQ_L \tag{3.12}$$

For an expected service life of N years, the total expected flood damage over this period can be discounted to a single present worth value as

$$D_P = D_A \cdot \text{pwf}(r\%, N) \tag{3.13}$$

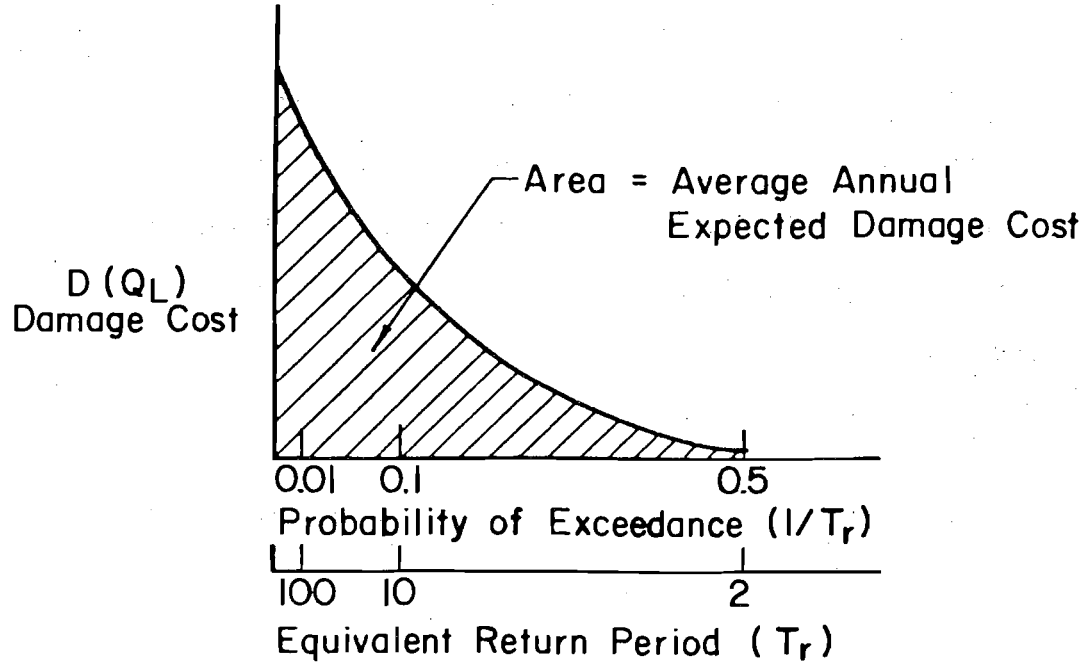

(a) For One Diameter

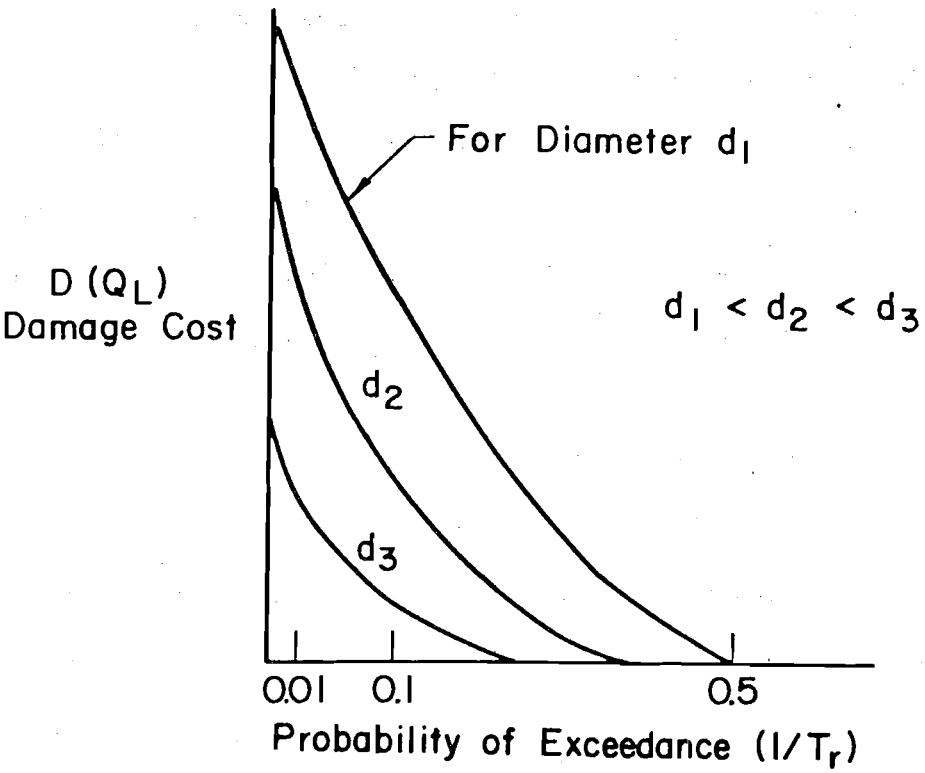

(b) For Various Diameters

Figure 3.4 Damage-Frequency Curves

where D_P is the present value of flood damage and pwf(r%,N) is the uniform series present worth factor for an interest rate of r% per year and a time period of N years. The expected total cost associated with a particular pipe design (diameter and slope) is simply the sum of D_P and the installation cost of the pipe.

The above procedure of computing D_A and D_P can be repeated for several commercial pipe sizes maintaining the same slope. For each pipe size the total expected cost, i.e., D_P plus installation cost, is computed. The pipe size corresponding to the minimum total expected cost is then selected as the best for the particular slope. The resulting damage-frequency curves for three diameters assuming the same pipe slope are shown in Fig. 3.4b. It is obvious that as the diameter increases the annual expected damages decrease; however, the installation cost of the sewer pipe increases as the diameter increases. It is through this trade-off that a proper balance can be maintained between the installation cost and potential flood damage costs. This procedure of accounting for potential flood damages has been used in conjunction with an optimization procedure as briefly described in the following chapter such that minimum cost designs of sewer systems can be achieved.

Using this double-integration approach, an example of a least-cost sewer design for the drainage basin given in ASCE Manual 37 has been presented in Tang et al.[13]

3.5. Estimation by Single Integral

In spite of the simplicity in form of Eq. 3.4, the computation involving double integration to obtain the expected annual damage cost is tedious and costly because of the repeated calculations for various combinations of $\bar{Q}_L$ and $\bar{Q}_C$ for each pipe size and location. Therefore, a simpler approximation involving only single integration is developed.

Assuming both Q_L and Q_C to be lognormal random variables, the ratio Q_L/Q_C will also be lognormally distributed with the mean and standard deviation of $\ell n(Q_L/Q_C)$ as

$$\lambda_{LC} = \lambda_{QL} - \lambda_{QC} \tag{3.14}$$

$$\delta_{LC} = (\delta_{QL}^2 + \delta_{QC}^2)^{\frac{1}{2}} \tag{3.15}$$

If the damage function, D, can be expressed in terms of $z = Q_L/Q_C$ only, then the expected annual damage given previously by Eq. 3.4 can be evaluated from a single integral as

$$D_A = E(D) = \int_1^\infty D(z)\ f(z)\ dz \tag{3.16}$$

in which

$$f(z) = \frac{1}{\sqrt{2\pi}\ \delta_{LC}\ z}\ \exp\left[-\frac{1}{2}\left(\frac{\ell n\, z - \lambda_{LC}}{\delta_{LC}}\right)^2\right] \tag{3.17}$$

For instance, consider the hypothetical sewer design of the ASCE Basin given in Tang et al.[13] as an example. For the case of a structure unit value equal to \$75,000, the coefficients in Eq. 3.1 are a = 0.92 and b = 6800 (Fig. 3.3). Hence, for rainfall duration t_d = 10 min and assuming for the triangular inflow hydrograph $t_b = 2\ t_d$, Eq. 3.3 can be rewritten, with damage costs in dollars, as

$$D(Q_L, Q_C) = 552\ Q_C \frac{[(Q_L/Q_C) - 1]^2}{Q_L/Q_C} + 6800 \tag{3.18}$$

where Q_L and Q_C are in cfs. Although Eq. 3.18 indicates that the damage D cannot be expressed in terms of Q_L/Q_C only, the ratio Q_L/Q_C is a dominant variable in the damage expression. The next step is to explore the possibility

of an approximate expression of damage D in terms of Q_L/Q_C.

For the optimal design of a given pipe in the DDDP approach, the mean inflow $\bar{Q}_L$ is known. The likely values of Q_L associated with that pipe would perhaps range from $\bar{Q}_L/2$ to $3\bar{Q}_L$ (this corresponds to a range of -2 to +8 times of standard deviations from the mean). At the same time, the range of likely values of Q_C for that pipe may be assumed to be between $\bar{Q}_L/2$ and $5\bar{Q}_L$ (assuming a maximum safety factor value of 2 to 3). Therefore, instead of establishing the approximate function D over all possible combinations of Q_L and Q_C for the entire storm sewer network, it would be more accurate to establish the approximate function $D(Q_L/Q_C)$ for a given value of $\bar{Q}_L$.

The procedure of establishing the approximate function $D(Q_L/Q_C)$ is as follows:

(i) Select the level of $\bar{Q}_L$, e.g., $\bar{Q}_L$ = 2 cfs

(ii) Establish the likely value of Q_L and Q_C based on $\bar{Q}_L/2 \leq Q_C \leq 5\bar{Q}_L$, and $\bar{Q}_L/2 \leq Q_L \leq 3\bar{Q}_L$. For $\bar{Q}_L$ = 2 cfs, $1 \leq Q_L \leq 5$ and $1 \leq Q_C \leq 10$

(iii) Select an appropriate increment Δ for Q_L and Q_C

(iv) Based on the domains of Q_L and Q_C in (ii) and the increment Δ in (iii), list all possible combinations of Q_L and Q_C. Since there will be no flood when $Q_L/Q_C < 1$; and $Q_L/Q_C > 4$ denotes an extremely rare event, those combinations having the ratio Q_L/Q_C and falling in these two ranges will be ignored.

(v) For each combination (Q_L, Q_C) identified in (iv), calculate the damage D according to Eq. 3.3 or Eq. 3.18 and also calculate the ratio Q_L/Q_C.

(vi) Plot D vs. Q_L/Q_C for all possible combinations (Q_L, Q_C) identified in (iv).

(vii) Through regression analysis establish the damage cost, D, as a function of Q_L/Q_C.

Table 3.1 summarizes the different levels of $\bar{Q}_L$ for which approximate expressions of $D(Q_L, Q_C)$ are determined, together with the range of values of Q_L, Q_C, and the increment Δ used in each case. For each level of $\bar{Q}_L$, the damage values are plotted against the ratio Q_L/Q_C as shown in Figs. 3.5(a) through (g). In all cases, a linear relation appears to fit the data points. A linear regression analysis is performed for each graph to establish the approximate relationship between the damage cost and Q_L/Q_C, i.e.,

$$D(Q_L,Q_C) \approx D(Q_L/Q_C) = c + m\ (Q_L/Q_C) \tag{3.19}$$

The results of the linear regression analysis for different $\bar{Q}_L$ are summarized in Table 3.2. Since the correlation coefficients are at least 0.78 for all cases, the error in using the regression line as the approximate formula of D is expected to be small.

In actual application, the values of $\bar{Q}_L$ at each pipe stage will generally not be exactly those listed in Tables 3.1 and 3.2. In order to establish a general expression of the damage cost as a function of Q_L/Q_C for any given value of $\bar{Q}_L$, the coefficients c and m in Eq. 3.19. may be expressed as a function of $\bar{Q}_L$. By plotting the values of the intercept c and $\bar{Q}_L$ from Table 3.2, a linearly decreasing trend may be visualized in Fig. 3.6. Performing a linear regression analysis again, the coefficient c can be predicted for a given value of $\bar{Q}_L$ as

$$c = 6956 - 157\ \bar{Q}_L \qquad 2 \leq \bar{Q}_L \leq 50 \tag{3.20}$$

The correlation coefficient between c and $\bar{Q}_L$ is computed to be 0.978, implying that the error in using Eq. 3.20 will be small. Similarly, linear regression analysis based on the data for m in Table 3.2 plotted on Fig.

TABLE 3.1. Ranges on Q_C and Q_L for Approximate Damage Cost Function Determination

$\bar{Q}_L$ cfs	Range of Q_L cfs	Range of Q_C cfs	Increment Δ cfs
2	1 to 5	1 to 10	1
5	2 to 14	2 to 24	2
10	5 to 30	5 to 50	5
20	10 to 60	10 to 100	10
30	15 to 90	15 to 150	10
40	20 to 120	20 to 200	10
50	25 to 145	25 to 245	20

TABLE 3.2. Linear Regression Results for D vs. Q_L/Q_C for Different $\bar{Q}_L$

$\bar{Q}_L$ cfs	Damage Intercept c	Slope m	Correlation Coefficient
2	6395	403	0.985
5	6201	706	0.790
10	4674	1975	0.814
20	4961	2488	0.785
30	2672	4463	0.827
40	285	6729	0.909
50	-1147	8100	0.905

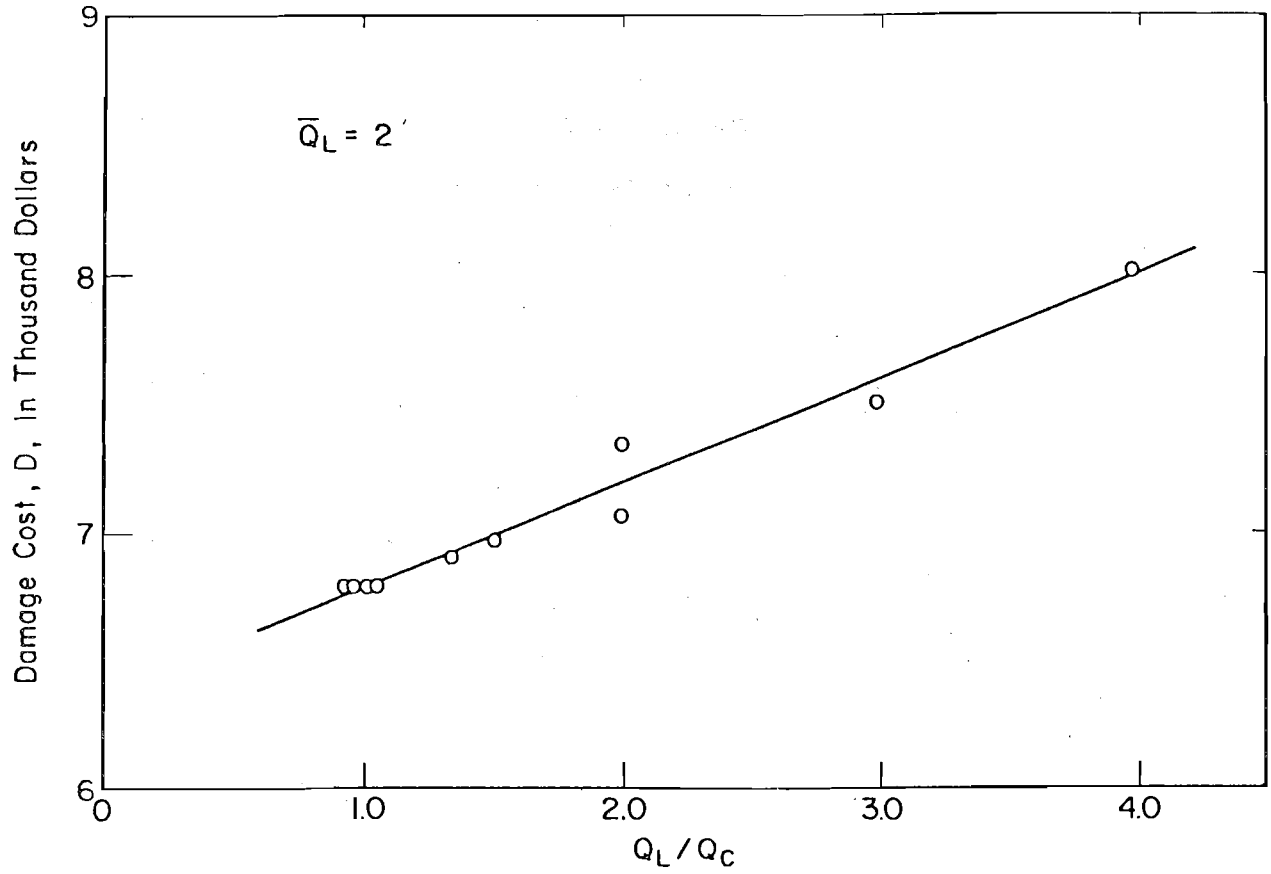

(a)

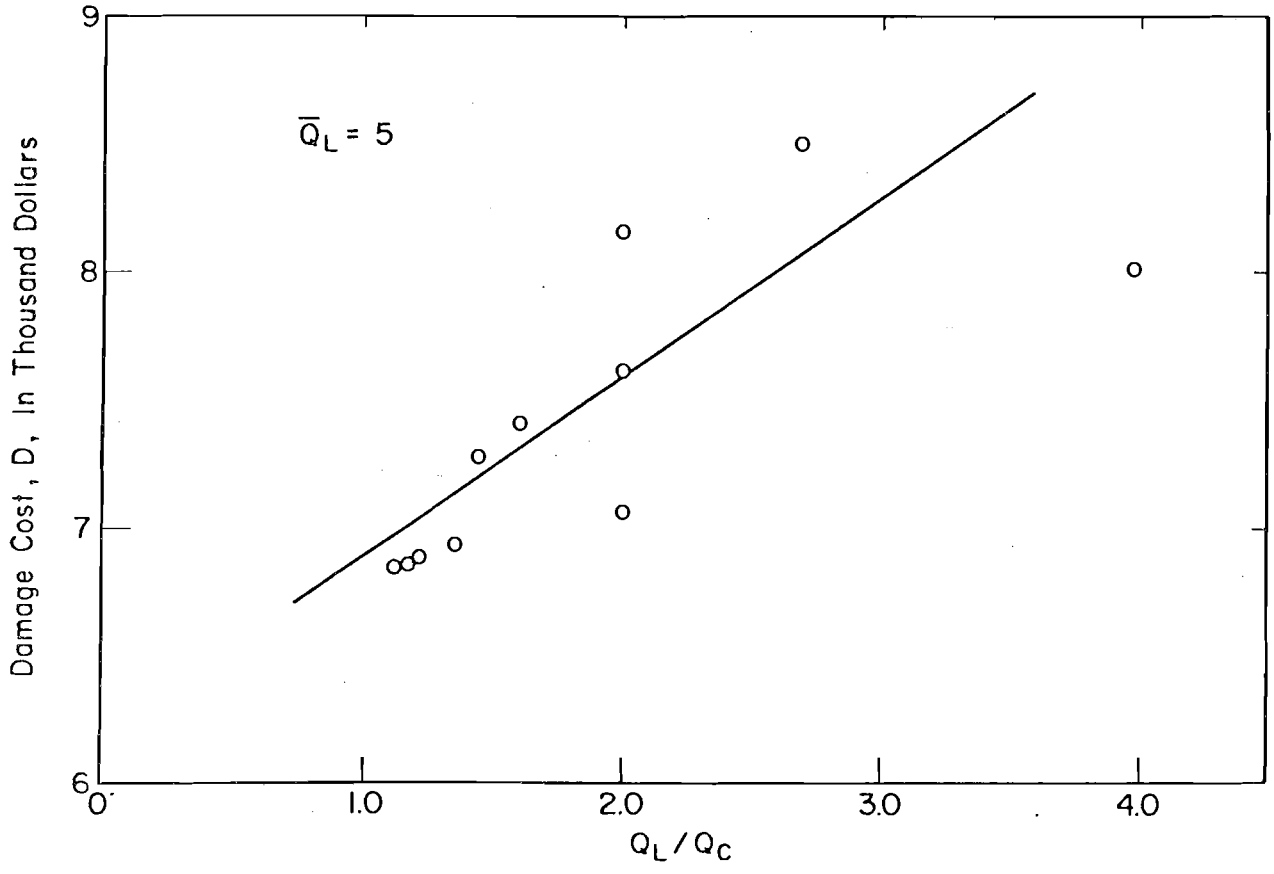

(b)

Figure 3.5 Damage Cost vs. Q_L/Q_C for Specified Value of $\bar{Q}_L$

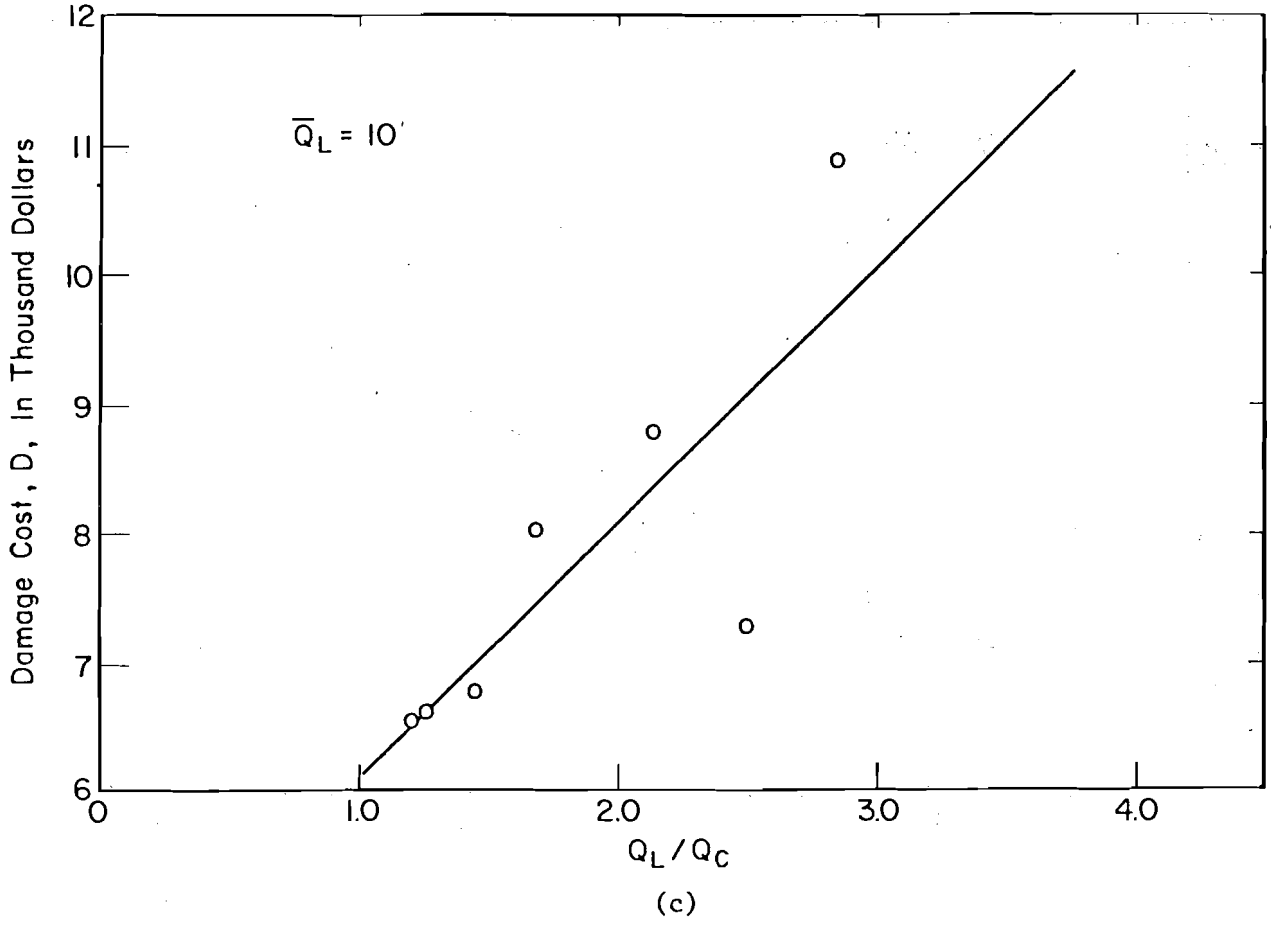

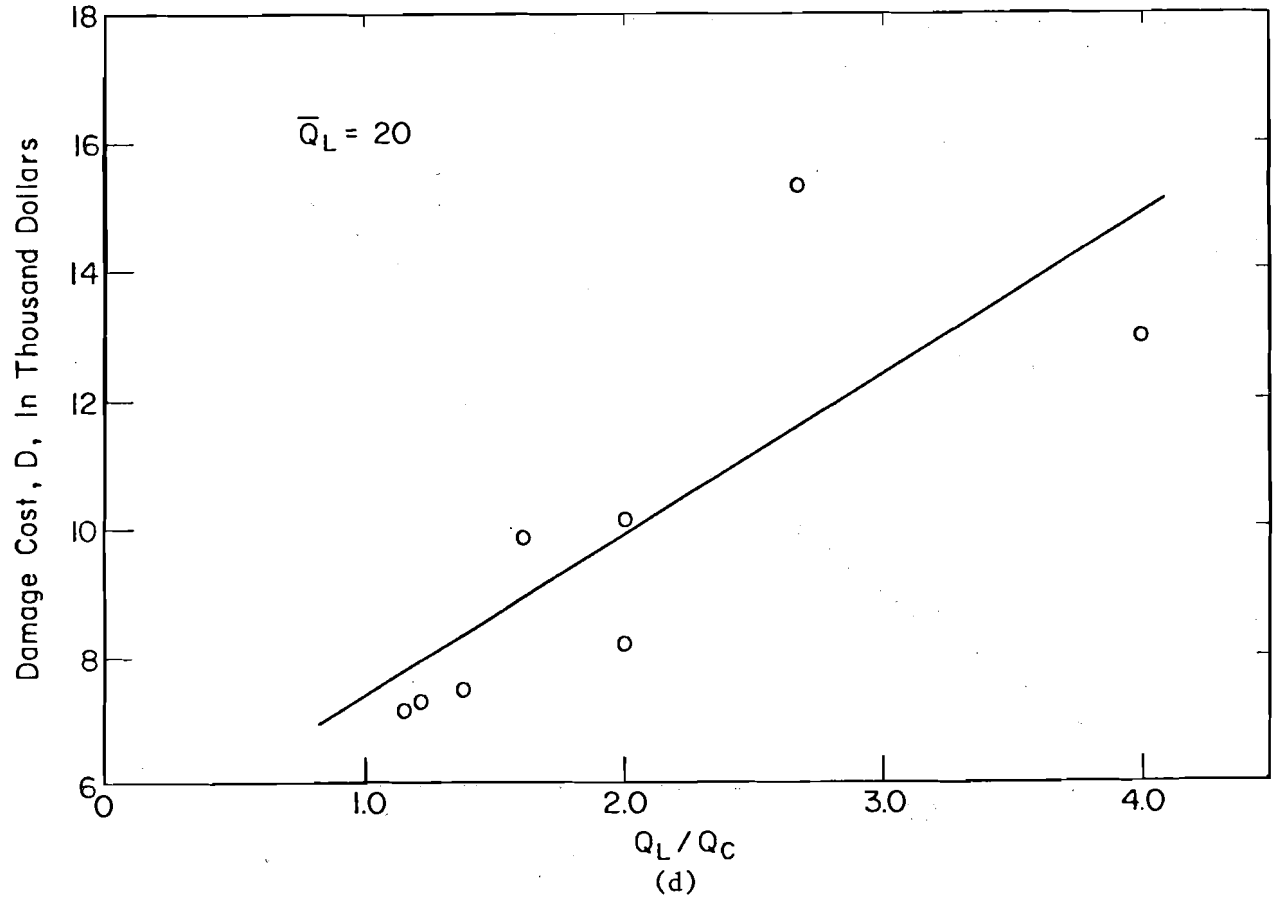

Figure 3.5 Damage Cost vs. Q_L/Q_C for Specified Value of $\bar{Q}_L$

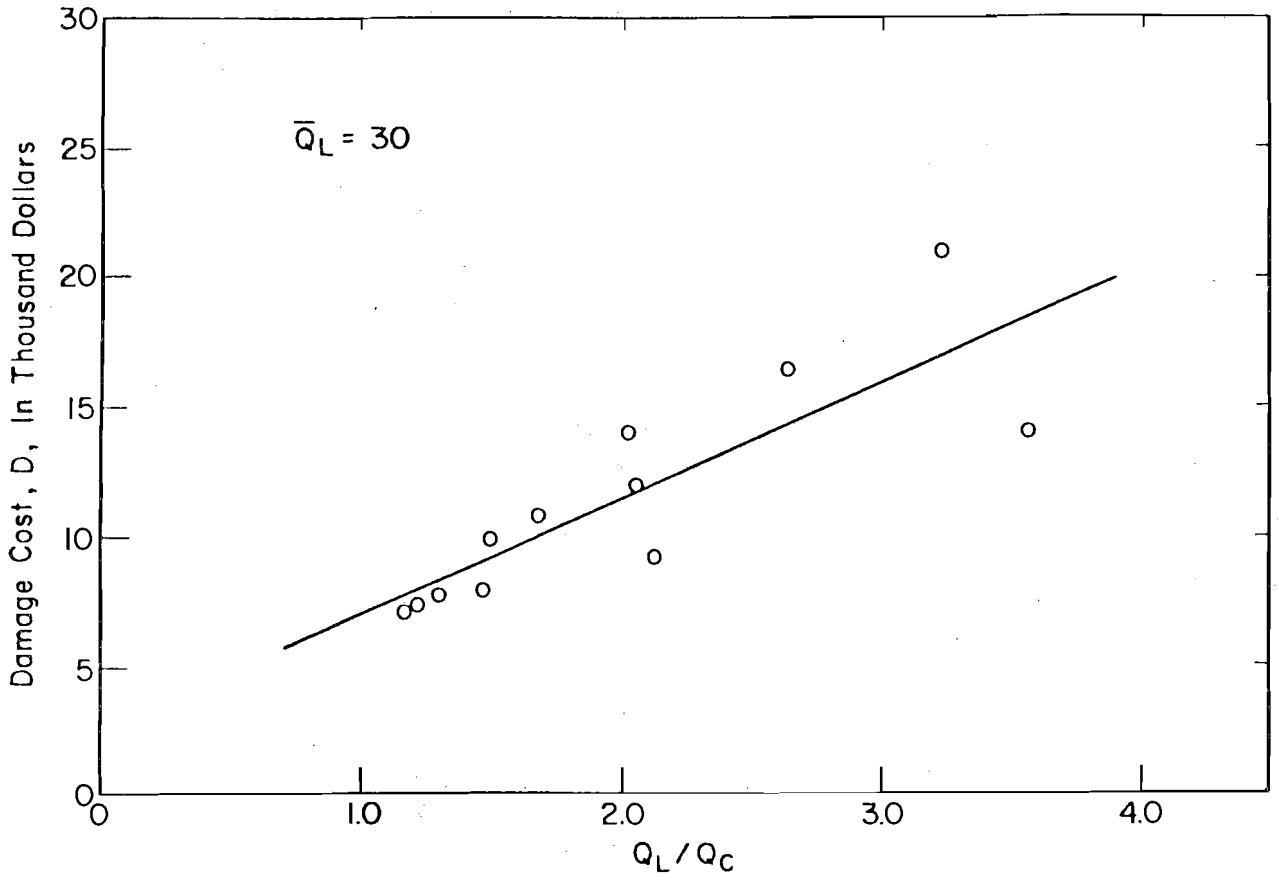

(e)

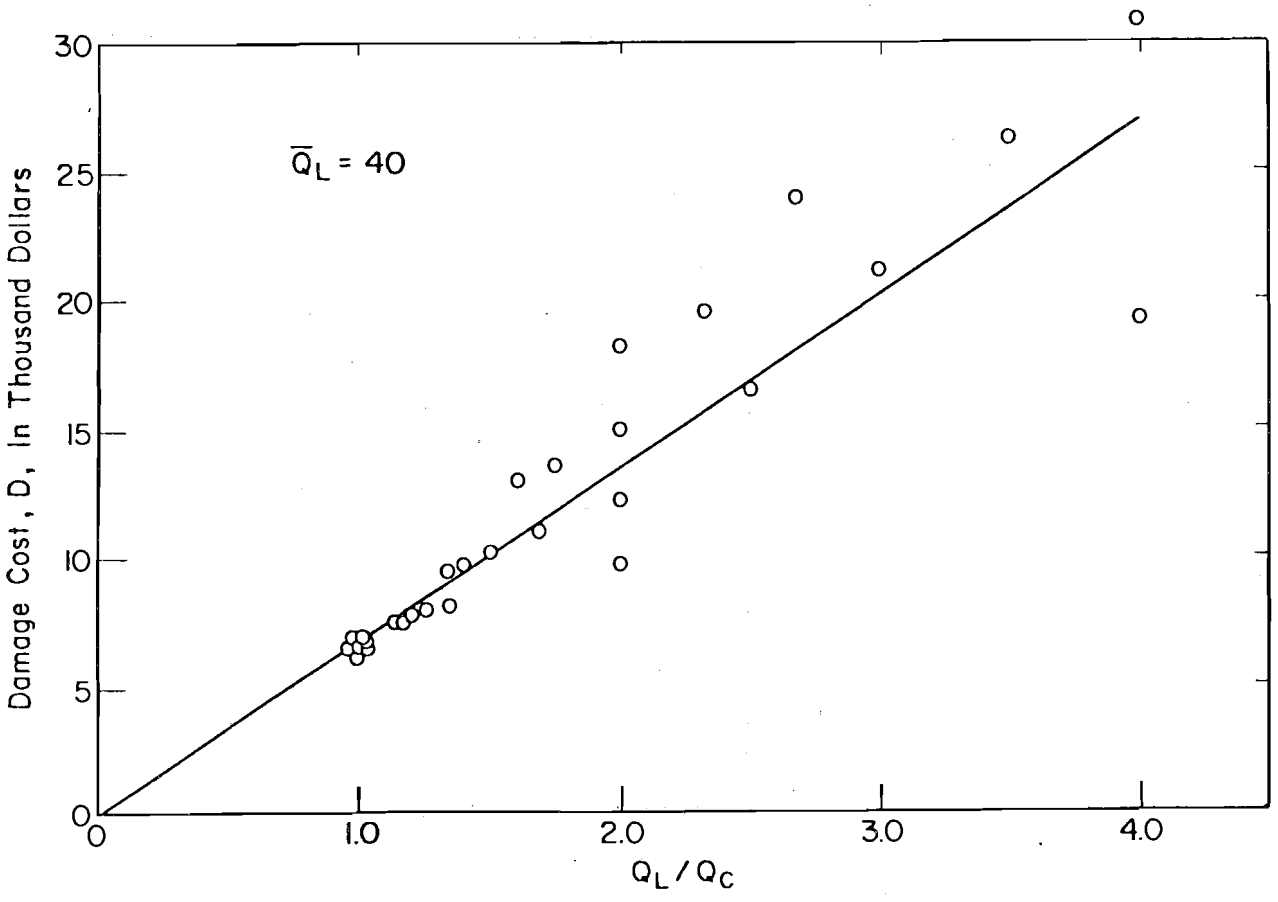

(f)

Figure 3.5 Damage Cost vs. Q_L/Q_C for Specified Value of $\bar{Q}_L$

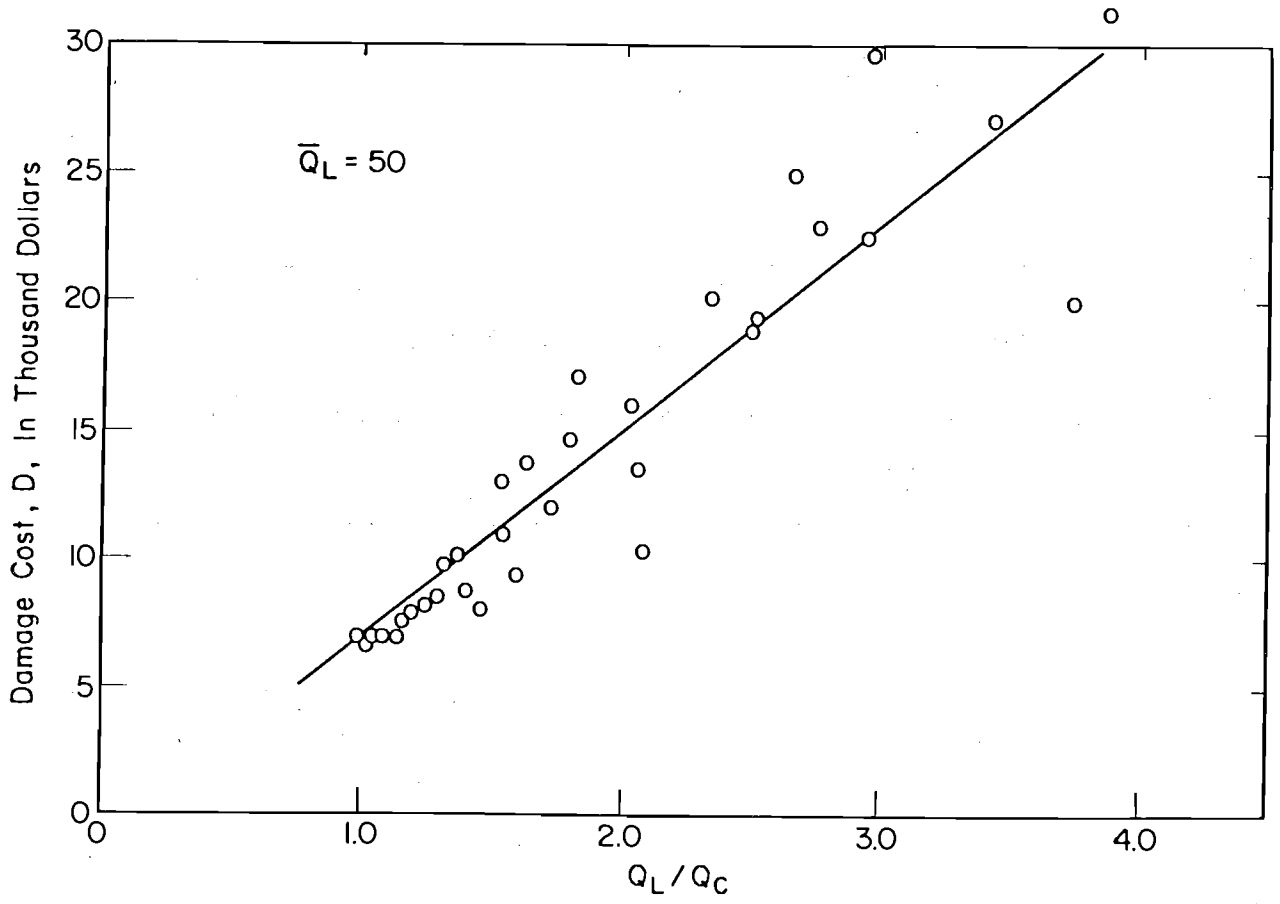

(g)

Figure 3.5 Damage Cost vs. Q_L/Q_C for Specified Value of $\bar{Q}_L$

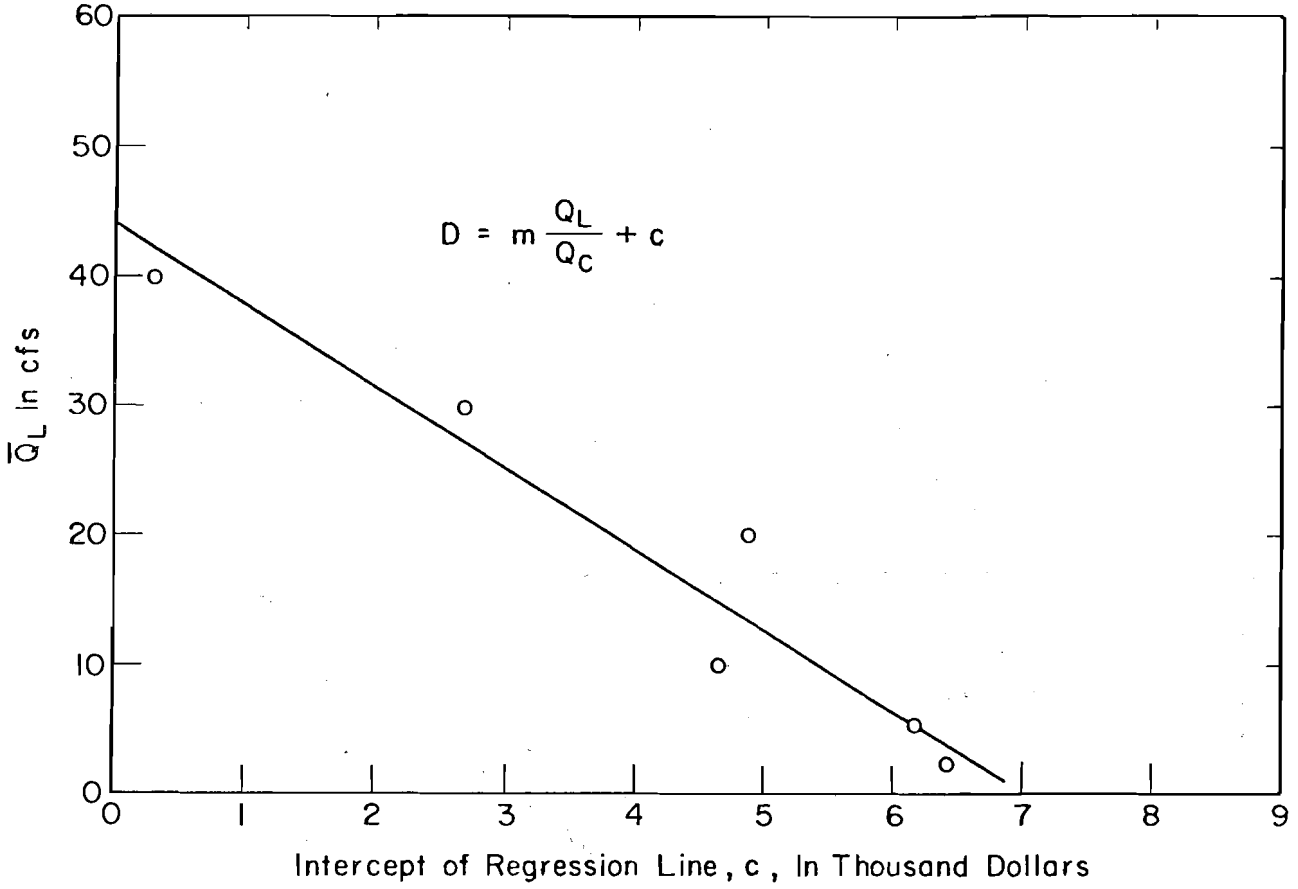

Figure 3.6 Variation of Regression Line Intercept with $\bar{Q}_L$

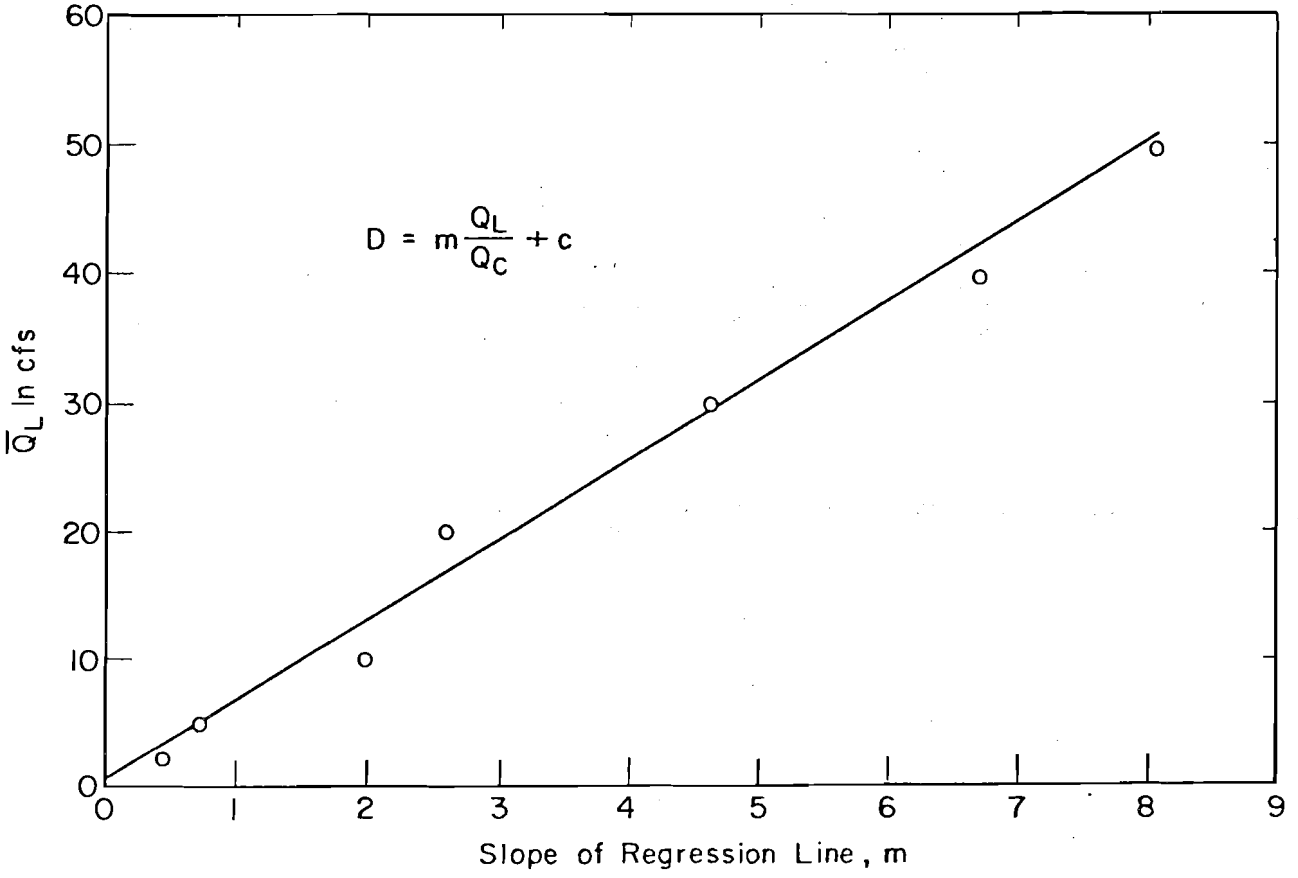

Figure 3.7 Variation of Regression Line Slope with $\bar{Q}_L$

3.7 yields

$$m = -70 + 161.5\,\bar{Q}_L \qquad 2 \leq \bar{Q}_L \leq 50 \tag{3.21}$$

with a correlation coefficient of 0.992.

Based on the approximated damage function $D(Q_L/Q_C)$ established in Eq. 3.19 with c and m from Eqs. 3.20 and 3.21, the expected annual flood damage can subsequently be computed from Eq. 3.16. For each pipe stage in the DDDP procedure, the mean inflow is known. Moreover, for each pipe size and slope considered, the mean flow capacity is also known. With given values of $\bar{Q}_L$ and $\bar{Q}_C$, the parameters λ_{LC} and δ_{LC} of the lognormal distribution of $z = Q_L/Q_C$ can be evaluated from Eqs. 3.14 and 3.15. For instance, for the hypothetical ASCE Basin sewer system which was designed using the double integral method by Tang et al.[13], with the example values of the coefficients of variation $\Omega_{QL} = 0.23$ and $\Omega_{QC} = 0.13$, from Eqs. 3.7 and 3.8,

$$\lambda_{QL} = \ell n \bar{Q}_L - 0.0265 \tag{3.22a}$$

$$\lambda_{QC} = \ell n \bar{Q}_C - 0.0085 \tag{3.22b}$$

and from Eqs. 3.14 and 3.15, noting that $\delta_{QL} \approx \Omega_{QL}$ and $\delta_{QC} \approx \Omega_{QC}$ for $\Omega < 0.3$,

$$\lambda_{LC} = \ell n(\bar{Q}_L/\bar{Q}_C) - 0.018 \tag{3.23a}$$

$$\delta_{LC} = 0.264 \tag{3.23b}$$

With these values of λ_{LC} and δ_{LC} the probability density function of $z = Q_L/Q_C$ is defined by Eq. 3.17. Subsequently, with f(z) from Eq. 3.17 and D(z) from Eq. 3.19, the approximate expected annual damage can be computed by using the single integral expression, Eq. 3.16. The computed results of D_A for the hypothetical example are given in Table 3.3.

TABLE 3.3. Comparison Of Expected Annual Damage Determined by Double Integration and Single Integral

$\bar{Q}_L$ cfs	$\bar{Q}_c$ cfs	D_A by Single Integral $	D_A by Double Integration $	Difference (Single-Double)/Double %
	1.5	5967.29	6009.13	-0.70
2	2	3381.01	3481.42	-2.88
	2.4	1456.48	1652.05	-11.84
	2.5	7517.93	7478.12	+0.52
5	5	3436.57	3528.91	-2.62
	6	1688.24	1677.71	+0.62
	5	8292.71	8190.77	+1.24
10	10	3518.75	3607.53	-2.46
	12	1714.28	1617.22	+6.03
	10	10044.74	9709.04	+3.46
20	20	3716.11	3767.44	-1.36
	24	1779.75	1757.09	+1.29
	15	11624.23	11088.11	+4.84
30	30	3902.27	3923.67	-0.55
	36	1840.66	1809.08	+1.75
	20	13266.35	12549.22	+5.71
40	40	4088.44	4083.10	+0.13
	48	1901.57	1862.13	+2.12
	25	14908.47	13977.47	+6.66
50	50	4274.60	4238.94	+0.84
	60	1962.49	1914.00	+2.53

These results can be compared to those obtained from double integration which are also listed in Table 3.3. The percentage difference of D_A computed by using the two different methods is generally small, mostly less than 10%. Hence the approximate single integral expression for the expected annual flood damage is adopted for further analysis in the DDDP procedure for optimal design of storm sewer system.

CHAPTER 4 SURFACE RUNOFF DETERMINATION

The ILSD models developed previously require the user to supply inlet hydrographs at each manhole. The development of these hydrographs was the responsibility of the user. In this phase of investigation an optional surface runoff calculation has been added to generate inlet hydrographs from the rainfall. The procedure is essentially the surface runoff portion of the Illinois Urban Drainage Area Simulator (ILLUDAS) model developed at the Illinois State Water Survey (Terstriep and Stall, 1974). This surface runoff model was adopted because of its relative simplicity and practicality in terms of requirements in data and computer time. Other surface runoff models can be added if it is deemed appropriate.

4.1 Basic Formulation

The surface runoff model is based on the time-area or isochrone concept. In this approach the catchment is divided into a series of zones bounded by lines of equal travel time to the outlet as shown in Fig. 4.1a. A graph of contributing area as a function of time can then be plotted as shown in Fig. 4.1b.

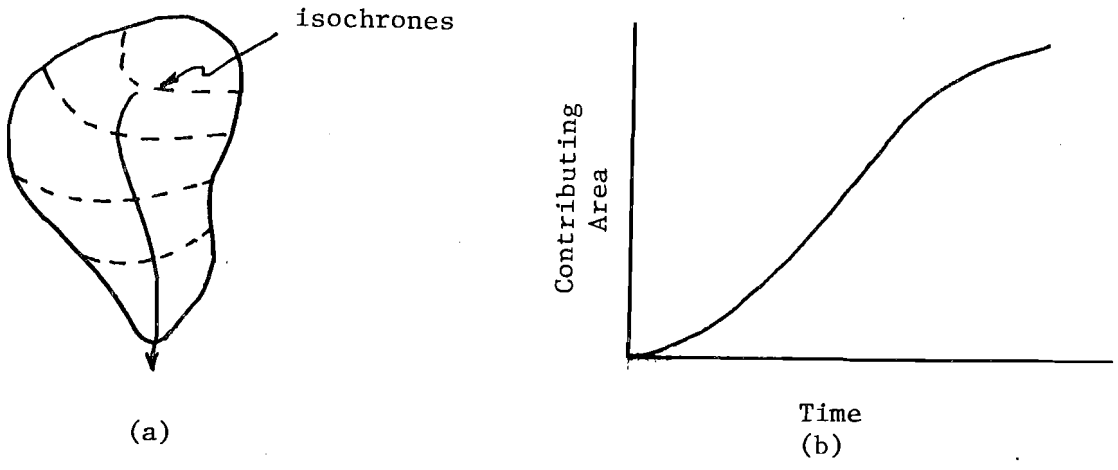

Fig. 4.1 Time-Area Diagram

The runoff hydrograph ordinate Q_j at any time t_j is given by

$$Q_j = \sum_{k=1}^{j} i_k \, \Delta A_{(j+1-k)} \qquad (4.1)$$

where i is the rainfall excess rate (rainfall which becomes surface runoff) in time interval k and ΔA is the incremental area between isochrones. Details of the surface runoff model can be found in Terstriep and Stall (1974).

4.2 ILLUDAS Hydrograph Generation

The surface runoff hydrograph generation procedure for a catchment considers the combined runoff hydrograph to be made up of the runoff hydrograph from paved areas and pervious areas. The time-area method is applied to the paved and pervious areas to generate the corresponding hydrographs separately and then they are combined together as the inlet hydrograph. The pervious area hydrograph includes the runoff from impervious areas which drain to pervious areas before reaching the catchment outlet. The procedure is described below.

4.2.1 Impervious Area Hydrograph

The application of Eq. 4.1 requires that the precipitation excess be determined and a time-area relationship be developed. The time-area relationship is determined for the impervious area by first calculating the total impervious area which drains directly to the sewer inlet without encountering any pervious surfaces. This would include streets, driveways, parking lots and roofs which do not drain onto pervious surfaces. The total travel time from the furthest point of the paved area from the inlet is then determined. The time-area curve is then assumed to be linear and defined by the origin and the point defined by the total paved area and its time of concentration.

The time of concentration can be estimated independently or computed within the model. The model uses Manning's formula to estimate a gutter flow velocity and adds to the gutter flow time an estimated paved area overland flow time of 2.0 min.

$$V = \frac{1.49}{n} R^{2/3} S^{1/2} \qquad (4.2)$$

in which R is the hydraulic radius of the gutter flow and is taken as 0.2 ft; n is Manning's roughness factor taken as 0.02, and S is the gutter slope. The gutter flow time is then computed as the gutter length divided by V.

For the impervious area the only abstractions utilized are initial losses, i.e., interception and depression storage. These are assumed to be satisfied at the beginning of the rainfall, after which the rainfall excess rate is assumed equal to the total rainfall rate. The hyetograph can be supplied independently or a total rainfall depth and duration provided with the hyetograph being computed within the model using a built-in distribution developed from Illinois storms.

4.2.2 Pervious Area Hydrograph

As with the impervious area, the time-area relationship is again assumed to be linear. The end point of the graph is the total pervious area contributing to flow at the sewer inlet and the time of concentration of this area. This time of concentration can be estimated independently or within the model using Izzard's formula (1946) with the roughness coefficient equal to 0.05 and rainfall intensity i = 1.0 in./hr. Under these conditions Izzard's formula is given by

$$t_e = 2.08 \left(\frac{L}{S}\right)^{1/3} \qquad (4.3)$$

in which t_e is the time of equilibrium in min for the pervious overland flow surface; L is the length of overland flow in ft, and S is the slope of the pervious surface. The total time of concentration is then the sum of t_e as computed above and the time of concentration for the paved area.

The effective rainfall is the total rainfall less abstractions. In this case the total rainfall for the pervious area is increased above the actual rainfall to account for runoff from impervious areas which drain into the pervious areas (termed supplemental impervious area). Drainage onto the pervious area is assumed to occur instantaneously and uniformly thereby effectively increasing the original total rainfall on the pervious area. The amount of the increase is equal to the ratio of the supplemental impervious area to the pervious area. The total rainfall for the pervious area is therefore given by

$$TR_j = R_j \ (1 + SIA/PA) \qquad (4.4)$$

where TR_j is the total rainfall for time increment j, R_j is the actual rainfall on the catchment during time increment j, SIA and PA are the supplemental impervious area and pervious area respectively. This total rainfall hyetograph is then used as the basis and abstractions are deducted to obtain the rainfall excess hyetograph.

4.2.3 Pervious Area Abstractions

Pervious area abstractions include interception, depression storage and infiltration. The first two are assumed to be satisfied before any rainfall

is available for infiltration. A value of 0.2 in. is the default value for the initial abstractions for the pervious area but any value can be specified.

The infiltration model is based on the Horton equation

$$f = f_c + (f_o - f_c)e^{-kt} \tag{4.5}$$

where f is the infiltration capacity, f_o and f_c are the initial and final capacities, respectively, k is a decay factor and t is time. This model was adopted after analysis of field data using methodology described by Holton (1961).

Values of f_o and f_c in Eq. 4.5 are selected according to soil type and five-day antecedent precipitation. The value of k used in the model is 2.0 hr^{-1}. Table 4.1 describes the four antecedent moisture conditions used.

Table 4.1 ILLUDAS Antecedent Moisture Conditions

AMC Designation	Description	5-Day Antecedent Precipitation (in.)
1	Bone dry	0
2	Rather dry	0-0.5
3	Rather wet	0.5-1.0
4	Saturated	>1.0

The values of f_o and f_c used in ILLUDAS are shown in Table 4.2.

Table 4.2 ILLUDAS Infiltration Parameters

SCS Hydrologic Soil Group	Description	f_c (in./hr)	f_o (in./hr) for AMC Designation 1	2	3	4
A	High infiltration rates (sand and gravel)	1.0	10.0	6.49	3.33	1.32
B	Moderate infil. rates and moderately well drained	0.5	8.0	5.23	2.63	1.18
C	Slow infil. rates	0.25	5.0	3.10	1.37	0.28
D	Very slow infil.rates (clays with permanent high water table and high swelling potential)	0.10	3.0	1.66	0.28	0.10

For each hyetograph time increment the infiltration capacity is computed using Eq. 4.5. If the rainfall intensity i is equal to or greater than f the effective rainfall rate is i - f. If f exceeds i then the effective rainfall is zero for that increment and the infiltration capacity during that increment is decreased such that the total incremental infiltration and rainfall depths are equal. This establishes a new value of f at the end of the time increment so that in effect t in Eq. 4.5 no longer corresponds to real time.

After the rainfall excess hyetograph for the pervious area is determined the time-area relationship is applied according to Eq. 4.1 to obtain the pervious area runoff hydrograph.

4.2.4 Total Runoff Hydrograph

The pervious and impervious area hydrograph ordinates are both computed using a common time scale with the same time increment. The total runoff hydrograph is simply their sum. This process is repeated for each sewer

inlet in the design. The abstractions can be varied with each sub-basin and the rainfall excess hyetograph can also be varied, but only in constant proportion to the original specified hyetograph.

The inlet hydrograph, whether produced by the surface runoff option or supplied by the user, is described by an array of ordinates at a prescribed time interval. More than one outlet hydrograph can be provided at a given manhole and the time interval, which is fixed for a given manhole, can vary with manhole. This feature provides the flexibility of utilizing the inlet hydrographs generated from the ILLUDAS surface runoff model together with others which are externally determined. The ILSD models contain an interpolation procedure which converts all hydrograph arrays to a single time interval which is specified for sewer routing purposes.

CHAPTER 5. ADDITIONAL IMPROVEMENTS

In addition to the major additions to the model described in previous chapters, a number of additional changes have been made of a more minor nature. These changes increase the utility of the model from the user's viewpoint and are described in this chapter.

5.1 Isonodal Line Designation

The description of the system and the operation of the DDDP procedure is based on the isonodal line concept as summarized in Chapter 1. The previous version of the model required the user to describe the system layout in terms of isonodal lines. Although this description is not difficult, it does require the user to understand the concept. It is a concept which is necessary as far as internal program operation is concerned but is not used in conventional procedures and therefore poses an additional burden to the user.

To avoid the necessity of the user describing the layout in terms of isonodal lines, a subroutine has been written which internally establishes the isonodal line description. The user is required simply to number the manholes in an arbitrary way and to designate for each manhole the manhole number or numbers of the manholes immediately upstream.

This subroutine, which represents a valuable practical improvement in the model, was written by Dr. Larry W. Mays* who, as a graduate student, was involved in the initial development of the model. The authors wish to acknowledge this additional contribution by Dr. Mays and appreciate his continued interest in the study.

*Assistant Professor of Civil Engineering, The University of Texas at Austin

5.2 Installation Cost Data

The original model utilized a set of cost functions developed by Alan M. Voorhees and Associates in 1969. These functions determined the installation cost (materials plus excavation) of a pipe or manhole given the diameter and excavation depth. Recognizing that these functions were developed for a specific project at a specific time a more general approach was developed to provide the necessary cost data.

This approach utilizes cost tables. Three types of cost tables are utilized: pipe cost, excavation cost and manhole cost. Table 5.1 is an example of a pipe cost table. The cost per unit length of each size of pipe for each class is provided. Pipe class is a function of strength, with an allowable range of buried depth associated with each class. The depth range associated with each class is provided along with the cost table. The model then chooses a pipe from the appropriate class depending on the crown elevation at the downstream end of the pipe.

5.1 Example Unit Pipe Cost Table

Nominal Pipe Diameter in.	Class I	Class II	Class III	Class IV	Class V
8	$ 2.30				
10	2.50				
12	3.00	$ 3.40	$ 3.40	$ 3.40	$ 4.40
15	3.90	4.45	4.45	5.25	5.90
18	5.15	5.90	5.90	6.85	8.10
21		7.40	7.40	8.60	9.55
24		9.20	9.20	10.90	11.80
27		10.25	11.05	12.85	14.45
30		13.65	14.20	16.05	18.05
33		14.65	16.40	18.70	20.95
36		18.40	19.05	21.70	24.30
42		24.10	25.00	27.30	32.65
48		30.85	32.05	35.70	46.35
54		37.95	39.45	43.30	
60		45.90	52.00	54.30	
66		52.35	55.40	62.50	
72		61.65	65.75	74.20	
78		73.35	78.90	88.35	
84		89.20	96.10	102.25	
90		97.65	103.65		
96		108.40	115.40		

A typical excavation and manhole cost table is shown in Table 5.2. The unit excavation costs are provided for various ranges of buried depth. The cost per unit length of manhole is also provided as a function of depth. Of course the depth variation capability need not be used if constant unit costs are utilized.

TABLE 5.2 Example Unit Excavation and Manhole Cost Table

Depth ft	Excavation Cost $/cu yd	Manhole Cost $/ft depth
0-6	3.00	$100.00
6-9	4.00	$100.00
9-12	5.00	$125.00
12-15	6.00	$150.00

In computing the excavation volume the difference between the average ground and pipe invert elevations is used as the depth and the pipe diameter is used as the width. In computing the manhole depth the minimum invert elevation of any pipe at the manhole is used as the elevation of the bottom of the manhole.

This method of providing cost data is very appealing to the engineer since it is very close to the format that is commonly used in engineering practice.

5.3 Crown and Invert Elevation Constraints

In any layout there is the possibility that a pipe elevation limitation of some kind is required at one or more points. For example, the outlet invert may be required to be above a certain receiving water surface elevation or buried utility lines may constrain possible pipe elevations.

To account for at least some of the elevation constraints four types of constraint possibilities have been introduced.

(a) The crown elevation at either or both ends of any pipe can be fixed at a specified value.

(b) An upper limit on crown elevation can be specified.

(c) A lower limit on invert elevation can be specified.

(d) The crown elevation and the pipe diameter can be specified. This means that the design of this pipe has been done externally or it is an existing pipe.

The last of the above options permits the model to be used in situations where a portion of the layout already exists and the new design must connect to it. In that event it is possible that an existing pipe will not have sufficient capacity to carry the design flow. In this case temporary storage is introduced at the upstream end of the existing pipe. The flow in excess of the pipe capacity is temporarily stored and then released as shown in Fig. 2.2. Also in this case the general constraint of non-decreasing pipe diameter in the downstream direction is relaxed as is done for the case of detention reservoirs as described in Chapter 2.

5.4 Initial Negative Slope Check

The initial trial trajectory (set of pipe elevations) for the system is established by the ground surface elevations at the manholes, the minimum buried depth and the range of initial trial pipe elevations (state space). It is possible that the ground surface may have a negative slope between any two manholes, thereby creating an initial negative trial pipe slope. Previously the ILSD Model could not accept a negative slope for the initial trajectory. The user was required to specify an initial trajectory without negative slope to start the computations. To free the user from this burden a procedure has been

developed to check the initial trial slopes for the entire layout and to assign positive slopes to those pipes which do not initially have them.

The procedure (for pipes without elevation constraints) for slope adjustment is as follows:

(a) A range of possible slopes computed using Mannings equation.

$$S_{max} = \left(\frac{nV_{max}}{1.49}\right)^2 \left(\frac{4}{d_{min}}\right)^{4/3} \tag{5.1}$$

$$S_{min} = \left(\frac{nV_{min}}{1.49}\right)^2 \left(\frac{4}{d_{min}}\right)^{4/3}$$

where V_{max} and V_{min} are the maximum and minimum allowable velocities as specified by the user and d_{max} and d_{min} are the maximum and minimum pipe sizes used in the design.

(b) For a pipe with an initial negative slope (pipe A) the upstream pipe elevation is held fixed and S_{max} as computed above is used to estimate a new downstream pipe elevation. This elevation is used as the upstream elevation of the next downstream pipe (pipe B) and its slope is then checked.

(c) If the slope of pipe B is positive after adjustment the new slope values for both pipes A and B are accepted and the design procedure continued. If not the slope of pipe A is decreased by ΔS where

$$\Delta S = 0.1(S_{max} - S_{min}) \tag{5.2}$$

The slope of pipe B is again checked and if it is still negative the slope of pipe A is again decreased by ΔS. This process is repeated until pipes A and B have positive slopes or until the trial slope of A reaches S_{min}.

(d) If positive slopes cannot be found using the above procedure an error message is printed and the design procedure is stopped after all pipes in the system are examined for negative initial slopes.

It is recognized that the above procedure will not correct all possible negative slope situations. However, it will correct many, and as more experience with the model is reported, the procedure can be improved.

CHAPTER 6 DESIGN EXAMPLES

Examples of sewer designs for two drainage basins are presented in this chapter to demonstrate the various improvements in the model as discussed in previous chapters.

6.1 Description of Example Drainage Basins

Two example drainage basins have been chosen for demonstration. The first is a drainage basin taken from ASCE Manual of Engineering Practice No. 37*. This basin is chosen because of the wide distribution of this Manual. The second is a small system along Goodwin Avenue in Urbana, Illinois. It is chosen because the actual design data as constructed as well as detailed basin data are available. For each example basin designs using the ILSD Models under five different conditions are considered:

(a) Least-cost design without considering risk costs and detention storage.

(b) Least-cost design considering risk costs but not detention storage.

(c) Least-cost design with non-optimized detention storage

(d) Least-cost design with optimized detention storage using two different unit storage costs.

In these examples the cost schedule for the sewer pipes and manholes is in the cost tables given in Section 5.2.

The following data pertain to all of the examples:

---

* "Design and Construction of Sanitary and Storm Sewers," Manuals and Reports on Engineering Practice No. 37, American Society of Civil Engineers, 1970.

Minimum soil cover depth	-	3.5 ft
Maximum allowable pipe velocity	-	10 ft/sec
Minimum allowable pipe velocity	-	2 ft/sec
Minimum pipe diameter	-	12 in.
Number of elevation lattice points	-	7
Reduction rate of lattice point spacing	-	0.5
Minimum lattice point spacing	-	0.05 ft
Time increment	-	120 sec

6.1.1 ASCE Drainage Basin

The layout, inlet catchment boundaries, areas and surface contours of the example ASCE Basin are shown in Fig. 6.1 (a). The slopes and runoff coefficients shown were used in the rational method design as presented in ASCE Manual 37. Figure 6.1 (b) shows the layout with the arbitrary manhole numbering scheme used for all example applications of this basin in this chapter. The other pertinent data are shown in Table 6.1.

6.1.2 Goodwin Avenue Drainage Basin

Figure 6.2 shows the layout, contours and manhole numbering scheme for the example Goodwin Avenue Drainage Basin at Urbana, Illinois. Table 6.2 gives the length of sewers, ground elevations at manholes and drainage areas for the inlets.

6.2 Inlet Hydrograph Generation by ILLUDAS Surface Runoff Model

One of the newly incorporated options for inlet hydrograph specification in ILSD Models is through the use of the surface runoff portion of ILLUDAS to generate the inlet hydrographs from rainfall. In order to demonstrate the application of this option, inlet hydrographs are generated for the Goodwin Avenue

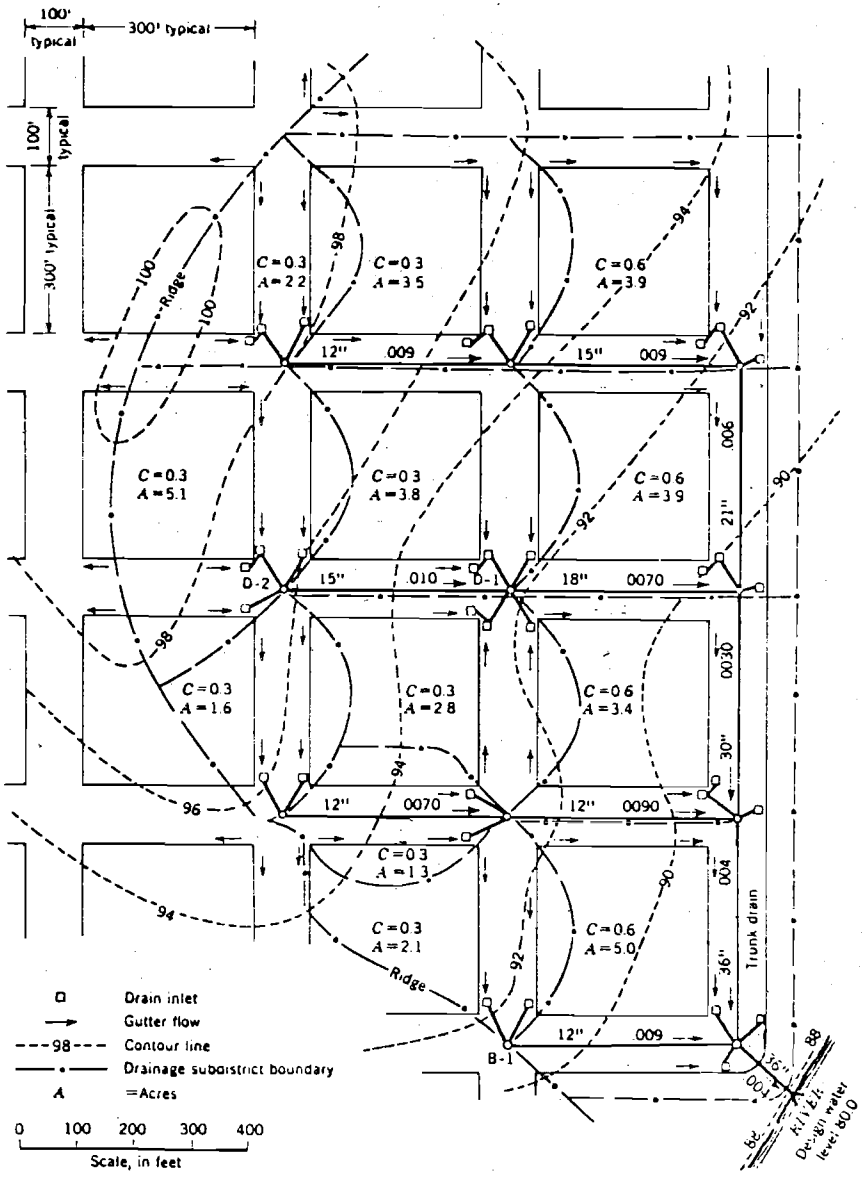

(a) Drainage Basin

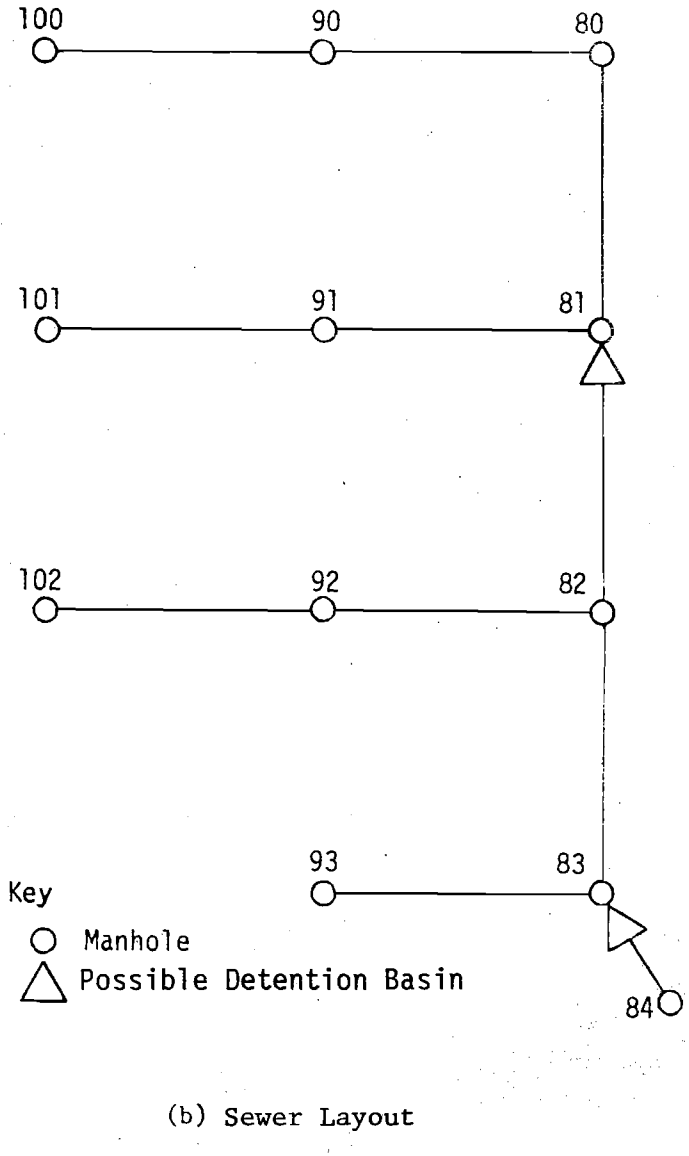

(b) Sewer Layout

Fig. 6.1 ASCE Drainage Basin

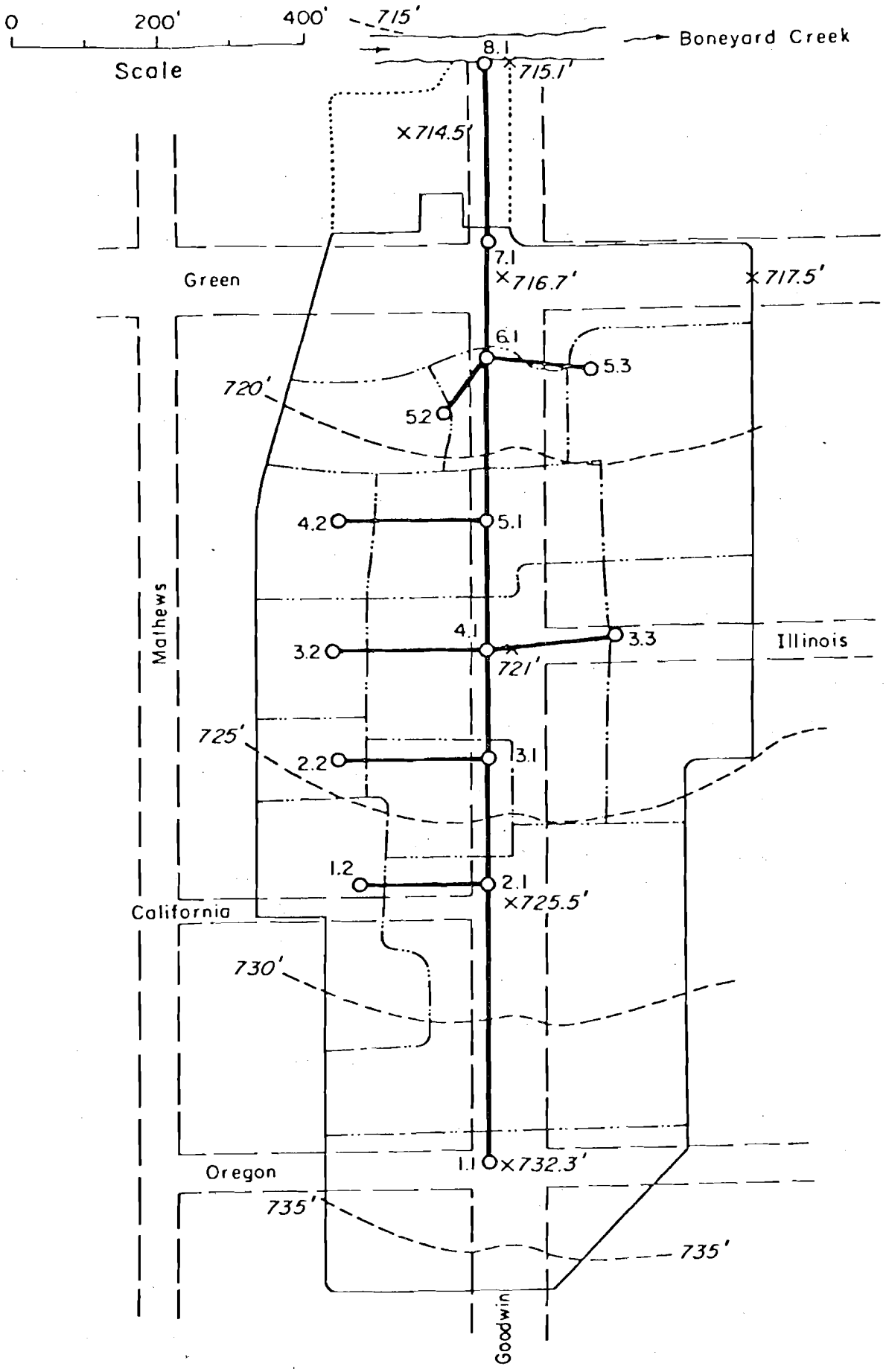

Fig. 6.2. Goodwin Avenue Drainage Basin at Urbana, Illinois

TABLE 6.1 - ASCE Drainage Basin

Manhole Number		Ground Elevation at Upstream Manhole	Sewer Length	Inlet Catchment Data		
Upstream	Downstream	ft	ft	Drainage Area ac	Coefficient C	Inlet Peak Flow Q_p cfs
100	90	98.4	400	2.2	0.3	2.0
90	80	94.9	400	3.5	0.3	3.1
101	91	96.2	400	5.1	0.3	4.6
80	81	91.8	400	3.9	0.6	6.8
91	81	92.3	400	6.6	0.3	5.7
102	92	94.6	400	1.6	0.3	1.5
81	82	89.7	400	3.9	0.6	6.5
92	82	92.7	400	1.3	0.3	1.1
82	83	89.5	400	3.4	0.6	5.6
93	83	91.6	400	2.1	0.3	2.0
83	84	88.5	125	5.0	0.6	8.1
84	*	88.0				

TABLE 6.2 - Goodwin Avenue Drainage Basin Data

Manhole Number		Ground Elevation at Upstream Manhole	Sewer Length	Drainage Area
Upstream	Downstream	ft	ft	ac
11	21	731.1	390	2.20
12	21	725.5	183	1.20
21	31	724.3	177	3.90
22	31	723.1	200	0.45
31	41	722.5	156	0.70
32	41	723.5	210	0.60
33	41	721.9	130	1.70
41	51	720.9	181	2.00
42	51	719.9	200	0.65
51	61	721.2	230	1.25
52	61	719.1	70	0.70
53	61	722.0	130	1.70
61	71	718.1	161	0.60
71	81	715.4	251	2.30
81		715.1		

Basin as an example. The design storm has a return period of 2 years, a duration of 20 minutes, and a rainfall depth of 1.03 in. The design hyetograph developed using the ILLUDAS optional built-in Huff rainfall temporal distribution and other pertinent data are shown in Table 6.3. The generated inlet hydrographs for each manhole are summarized in Table 6.4.

6.3 Examples Demonstrating Least-Cost Sewer System Design Without Detention Storage

Two examples are given in this section for each of the two drainage basins to illustrate the effect of the risk option on the design. No detention storage is considered in these examples. For each basin one example is the least-cost system design without considering the risk costs. For the ASCE Basin this is essentially the same as the corresponding design example reported in Yen et al. (1976) except that the cost tables given in Sec. 5.2 are used here instead of the cost functions used previously. The other example is the least-cost system design considering the risk costs as described in Chapter 2.

6.3.1 ASCE Basin Sewer Designs

In order to demonstrate the flexibility of the ILSD models in accepting inlet hydrographs in this example, triangular-shape inlet hydrographs are arbitrarily chosen, whereas in Section 6.3.2 ILLUDAS-generated inlet hydrographs are used for the Goodwin Avenue Basin. The peak discharges for the ASCE Basin are obtained based on the information given in ASCE Manual 37. This will provide some basis for comparison of the designs obtained from the proposed models with the design using the rational method as described in ASCE Manual 37. The inlet hydrographs are assumed to be triangular and symmetrical in shape, all starting at $t = 0$. The base time of the triangular bydrograph is 20 minutes. The peak inlet discharges are given in Table 6.1. No base flow is assumed. The installation cost data used in the design are given in Tables 5.1 and 5.2 and the risk costs were computed as described in Chapter 3. The only pipe elevation

TABLE 6.3 - Example Rainfall Input For Goodwin Avenue Basin

(a) Condition

Hyetograph Shape	HUFF
Rainfall Frequency (yr)	2.0
Rainfall Duration (min)	20.0
Antecedent Moisture Condition	4.
Input Time Interval of Hyetograph (min)	5.0
Initial Basin Paved Abstraction (in.)	0.10
Initial Basin Pervious Abstraction (in.)	0.20
Basin Hydrologic Soil Group	B

(b) Input Hyetograph

Time (min)	Incremental Rainfall (in.)
0	0.000
5	0.613
10	0.206
15	0.113
20	0.098

Total Rainfall = 1.03 in.

TABLE 6.4 - Example Inlet Hydrographs Generated For Goodwin Avenue Basin

Manhole No	(1) DCIA ac	(2) CPA ac	(3) SIA ac	(4) IIT min	(5) PIT min	Hydrograph Ordinates (cfs) at Times (min) 0	5	10	15	20	25	30	35	40	45	50	55
11	1.98	0	0	11.0	-	0	5.54	7.76	4.55	2.73	1.30	0.21	0				
12	0.96	0.12	0.12	9.2	29.7	0	3.40	4.25	2.10	1.55	0.85	0.34	0.34	0.30	0.14	0.06	0.03
21	1.56	1.17	1.10	11.0	20.0	0	6.67	9.34	7.32	6.31	5.19	4.33	2.32	1.12	0.53	0.09	0
22	0.45	0	0	5.2	-	0	2.66	1.18	0.63	0.53	0.02	0					
31	0.63	0	0	8.7	-	0	2.23	2.54	1.16	0.79	0.32	0					
32	0.60	0	0	5.9	-	0	3.13	1.82	0.92	0.72	0.11	0					
33	0.85	0.34	0.51	11.8	30.9	0	2.85	3.98	3.19	2.36	1.72	1.28	1.12	1.12	0.83	0.38	0.19
41	1.20	0.40	0.40	9.5	15.0	0	4.89	6.46	3.88	3.32	2.37	0.76	0.38	0.17	0		
42	0.65	0	0	6.2	-	0	3.23	2.07	1.02	0.79	0.15	0					
51	1.19	0	0	4.4	-	0	7.31	2.94	1.62	1.39	0						
52	0.70	0	0	11.8	-	0	1.83	2.56	1.79	1.02	0.49	0.13	0				
53	0.85	0.68	0	12.0	25.0	0	2.63	3.72	3.02	2.14	1.50	1.06	0.89	0.62	0.31	0.15	0.04
61	0.54	0	0	3.17	-	0	3.32	1.34	0.73	0.63	0.						
71	1.61	0.69	0	10.0	20.0	0	5.51	7.78	4.07	3.16	2.06	1.12	0.56	0.28	0.13	0	

Notes:

(1) DCIA = Directly Connected Impervious Area

(2) CPA = Connected Pervious Area

(3) SIA = Supplemental Impervious Area

(4) IIT = Impervious Area Inlet Time

(5) PIT = Pervious Area Inlet Time

TABLE 6.5 Comparison of Sewer Designs Without Detention Storage for ASCE Basin

Sewer Manhole No.		Design With Risk Cost Optimization						Design Without Risk Cost Optimization						Rational Method Design from ASCE Manual					
U/S	D/S	Invert Elev U/S ft	Invert Elev D/S ft	Slope %	Pipe diam in.	Risk cost $	Risk	Invert Elev U/S ft	Invert Elev D/S ft	Slope %	Pipe diam in.	Risk cost $	Risk	Invert Elev U/S ft	Invert Elev D/S ft	Slope %	Pipe diam in.	Risk cost $	Risk
83	84	80.56	80.05	0.410	42	222	0.209	81.44	80.93	0.410	36	4088	0.650	80.55	80.05	0.400	36	Surcharged	
82	83	81.56	80.56	0.250	42	342	0.226	82.50	81.44	0.266	36	3590	0.637	82.15	80.55	0.400	36	1388	0.461
93	83	87.10	83.13	0.994	12	0	0.077	87.10	84.00	0.775	12	207	0.145	84.55	80.55	0.900	12	62	0.100
81	82	83.20	82.06	0.284	36	858	0.350	83.20	82.50	0.175	36	3442	0.603	83.75	82.15	0.400	30	Surcharged	
92	82	88.07	84.06	1.003	12	321	0.311	88.20	85.00	0.800	12	796	0.450	85.75	82.15	0.900	12	567	0.387
80	81	86.30	84.20	0.525	24	328	0.244	86.55	84.45	0.525	21	3206	0.630	86.15	83.75	0.600	21	2545	0.562
91	81	86.43	84.20	0.556	24	38	0.112	87.05	84.45	0.650	21	1114	0.387	86.55	83.75	0.700	18	Surcharged	
102	92	90.10	88.08	0.506	12	62	0.101	90.10	88.20	0.475	12	123	0.116	88.55	85.75	0.700	12	0	0.040
90	80	89.71	86.80	0.728	18	0	0.081	90.15	87.05	0.775	15	1692	0.503	89.75	86.15	0.900	15	1273	0.451
101	91	91.45	87.18	1.069	15	394	0.208	91.45	87.55	0.975	15	677	0.255	90.55	86.55	1.000	15	570	0.241
100	90	93.90	90.21	0.922	12	38	0.094	93.90	90.40	0.875	12	90	0.108	93.35	89.75	0.900	12	62	0.100
					average		0.183				average		0.408						
		Installation cost = $49,197						Installation cost = $42,836						Installation cost = $42,235					
		Expected damage cost = $ 2,602						Expected damage cost = $19,025						Expected damage cost = $20,000					
		Total cost = $51,799						Total cost = $61,861											

TABLE 6.6 - Comparison Of Sewer Designs Without Detention Storage For Goodwin Avenue Basin

Sewer Manhole No. U/S	Sewer Manhole No. D/S	Design With Risk Cost Optimization: Invert Elev. U/S ft	Invert Elev. D/S ft	Slope %	Pipe diam in.	Risk Cost $	Risk	Design Without Risk Cost Optimization: Invert Elev. U/S ft	Invert Elev. D/S ft	Slope %	Pipe diam in.	Risk Cost $	Risk
71	81	707.28	704.04	1.290	36	1292	0.137	707.71	705.54	0.867	36	3925	0.332
61	71	709.35	707.28	1.289	36	433	0.078	708.73	707.71	0.629	36	4202	0.405
51	61	711.83	709.35	1.076	36	173	0.084	711.95	709.23	1.185	30	4087	0.494
52	61	714.60	713.41	1.696	12	0	0.011	714.60	713.60	1.429	12	90	0.020
53	61	717.50	712.73	3.673	12	0	0.033	717.50	713.60	3.000	12	162	0.061
41	51	713.71	711.83	1.043	36	0	0.047	714.96	712.20	1.526	27	3999	0.528
42	51	715.15	713.58	0.788	15	90	0.047	715.40	713.45	0.975	12	3401	0.470
31	41	715.91	714.21	1.133	30	39	0.056	716.04	714.96	0.717	27	3407	0.493
32	41	718.75	716.15	1.238	15	0	0.006	719.00	716.40	1.238	12	1679	0.229
33	41	717.15	715.46	1.298	15	0	0.140	717.15	716.15	0.769	15	676	0.430
21	31	718.55	716.16	1.349	27	92	0.076	718.80	716.60	1.243	24	2052	0.394
22	31	718.35	717.16	0.594	15	17	0.011	718.60	717.29	0.656	12	3392	0.242
11	21	726.10	719.30	1.744	18	17	0.018	726.35	719.55	1.744	15	2505	0.257
12	21	720.50	719.30	0.656	18	0	0.050	720.75	719.55	0.656	15	1684	0.454
						average	0.057					average	0.343
		Installation cost = $39,846						Installation cost = $34,133					
		Expected damage cost = 2,153						Expected damage cost = 35,260					
		Total cost = 41,999						Total cost = 69,393					

TABLE 6.7 - Comparison of Sewer System Designs With Detention Storage For ASCE Basin

Sewer Manhole No.		Design With Storage Not Optimized					Design With Storage Optimized									
							Storage cost=$0.50 per cu ft					Storage cost=$0.10 per cu ft				
U/S	D/S	Invert Elev. U/S ft	Invert Elev. D/S ft	Slope %	Pipe diam in.	Stor. vol ft^3	Invert Elev. U/S ft	Invert Elev. D/S ft	Slope %	Pipe diam in.	Stor vol ft^3	Invert Elev. U/S ft	Invert Elev. D/S ft	Slope %	Pipe diam in.	Stor vol ft^3
83	84	80.75	80.05	0.560	36	0	80.56	80.05	0.410	36	0	80.88	80.05	0.660	27	1055
82	83	81.50	80.75	0.188	36	0	81.31	80.56	0.188	36	0	82.25	80.88	0.344	27	0
93	83	87.10	84.00	0.775	12	0	87.10	84.00	0.775	12	0	87.10	84.00	0.775	12	0
81	82	83.95	82.25	0.425	27	2987	83.95	82.06	0.472	27	2188	84.45	82.75	0.425	21	13,672
92	82	88.20	85.00	0.800	12	0	88.20	85.00	0.800	12	0	88.20	85.00	0.800	12	0
80	81	86.55	84.45	0.525	21	0	86.55	84.45	0.525	21	0	86.55	84.45	0.525	21	0
91	81	87.05	84.45	0.650	21	0	87.05	84.45	0.625	21	0	87.05	84.45	0.650	21	0
102	92	90.10	88.20	0.475	12	0	90.10	88.20	0.475	12	0	90.10	88.20	0.475	12	0
90	80	90.15	87.05	0.775	15	0	90.15	87.05	0.775	15	0	90.15	87.05	0.775	15	0
101	91	91.45	87.55	0.975	15	0	91.45	87.55	0.975	15	0	91.45	87.55	0.975	15	0
100	90	93.90	90.40	0.875	12	0	93.90	90.40	0.875	12	0	93.90	90.40	0.875	12	0
		Installation cost =$39,894 Storage cost (0.50/ft^3) =$ 1,493 Storage cost (0.10/ft^3) =$ 299 Total cost (0.50/ft^3stor)=$41,387 Total cost (0.10/$ft^3$stor)=$40,193					Installation cost = $39,983 Storage cost = $ 1,094 Total cost = $41,076					Installation cost = $33,420 Storage cost = $ 1,473 Total cost = $34,893				

TABLE 6.8 - Comparison of Sewer System Designs With Detention Storage For Goodwin Avenue Basin

Sewer Manhole No. U/S	D/S	Design With Storage Not Optimized: Invert Elev. U/S ft	D/S ft	Slope %	Pipe diam. in.	Volume Storage ft^3	Design With Storage Optimized — Storage Cost = \$0.50 per cubic ft: Invert Elev. U/S ft	D/S ft	Slope %	Pipe diam. in.	Volume Storage ft^3	Storage Cost = \$0.10 per cubic ft: Invert Elev. U/S ft	D/S ft	Slope %	Pipe diam. in.	Volume Storage ft^3
71	81	709.46	705.66	1.514	27	0	707.59	705.60	0.792	36	0	710.09	704.66	2.161	21	0
61	71	711.04	709.46	0.978	27	0	710.60	708.09	1.561	30	0	711.60	710.09	0.939	21	0
51	61	712.20	711.04	0.505	27	13,126	713.14	710.60	1.103	30	273	712.95	711.85	0.478	18	30,352
52	61	714.60	713.60	1.429	12	0	714.60	713.60	1.429	12	0	714.60	713.60	1.429	12	0
53	61	717.50	713.60	3.000	12	0	717.50	713.60	3.000	12	0	717.50	713.60	3.000	12	0
41	51	714.96	712.20	1.526	27	0	714.71	713.14	0.870	30	0	714.96	712.20	1.526	27	0
42	51	715.40	713.45	0.975	12	0	715.15	714.51	0.319	15	0	715.40	713.45	0.975	12	0
31	41	716.04	714.96	0.717	27	0	716.04	714.96	0.717	27	0	716.04	714.96	0.717	27	0
32	41	719.00	716.40	1.238	12	0	719.00	716.40	1.238	12	0	719.00	716.40	1.238	12	0
33	41	717.15	716.15	0.769	15	0	717.15	716.15	0.769	15	0	717.15	716.15	0.769	15	0
21	31	718.80	716.60	1.243	24	0	718.80	716.60	1.243	24	0	718.80	716.60	1.243	24	0
22	31	718.60	717.29	0.656	12	0	718.60	717.29	0.656	12	0	718.60	717.29	0.656	12	0
11	21	726.35	719.55	1.744	15	0	726.35	719.55	1.744	15	0	726.35	719.55	1.744	15	0
12	21	720.75	719.55	0.656	15	0	720.75	719.55	0.656	15	0	720.75	719.55	0.656	15	0
		Installation cost = \$28,998 Storage cost (0.50/ft^3) = \$ 6,563 Storage cost (0.10/ft^3) = \$ 1,313 Total cost (0.50/ft^3 stor)=\$35,561 Total cost (0.10/ft^3 stor)=\$30,311					Installation Cost = \$33,669 Storage Cost = \$ 137 Total Cost = \$33,806					Installation Cost = \$25,694 Storage Cost = \$ 3,035 Total Cost = \$28,729				

constraint used was the invert elevation of the outlet pipe which was limited to a minimum of 80.05.

Design runs were made both with and without utilizing the risk costs options in the optimization procedure. The results of the designs are summarized in Table 6.5. Also summarized in Table 6.5 for comparison is the design based on the rational method as given in ASCE Manual 37.

6.3.2 Goodwin Avenue Basin Sewer Designs

As a further demonstration the sewer system for the Goodwin Avenue Basin is designed using the inlet hydrographs generated by the ILLUDAS surface runoff model which are listed in Table 6.4. It should be noted here that in using the surface runoff option of the ILSD Models, the design can be proceeded without printing out the inlet hydrographs if the designer has no interest in seeing them. The required soil data and other rainfall input information are given in Table 6.3. The results of the designs are summarized in Table 6.6.

6.4 Examples Demonstrating Least-Cost Design with Detention Storage

As discussed in Chapter 2, the proposed model has two options in regard to detention storage, depending on whether or not the storage volume cost is included in the optimization procedure. These two options are applied to both the ASCE and Goodwin Avenue basins. For the ASCE Basin again the triangular inlet hydrographs described in Section 6.3.1 are used whereas for the Goodwin Avenue Basin the ILLUDAS-generated inlet hydrographs (Table 6.4) are utilized.

6.4.1 Least-Cost Design Without Including Detention Storage Cost in Optimization

In this option the maximum allowable outflow from a reservoir into the sewer downstream is specified. The volume of storage that is required to satisfy this specified flow restriction is computed as well as its costs based on a unit storage cost specified by the user. However, these costs of storage are not considered in the optimization procedure.

For the ASCE Basin design, storage locations are specified downstream of manholes 81 and 83 (see Fig. 6.1). The maximum flow downstream of manholes 81 and 83 was limited to 20.0 cfs and 40.0 cfs, respectively. The result is summarized in Table 6.7. The storage cost is computed for unit costs of $0.50 as well as $0.10 per cubic ft.

For the Goodwin Avenue Basin examples, a single detention storage reservoir location is chosen which is downstream of manhole 51 (Fig. 6.2). The maximum outflow specified for the reservoir is 20.0 cfs. The result is summarized in Table 6.8.

6.4.2 Least-Cost Design with Storage Optimization

In this option the maximum allowable storage volume at a detention reservoir site is specified along with a unit storage cost. The cost of the storage is included with the other costs as part of the optimization procedure.

For the ASCE Basin, the locations of the reservoir sites are the same as in the previous section. The maximum allowable storage volumes downstream of manholes 81 and 83 are 14,000 and 22,500 ft^3, respectively. Table 6.7 shows the results of two designs using unit storage costs of $0.50 and $0.10 per cubit ft. As would be expected, lower unit storage cost resulted in more storage being utilized. The increase in storage costs was more than offset by the decrease in installation cost. Also note that the $48,857 total cost for the design using a unit storage cost of $0.50/$ft^3$ is less than the corresponding design shown in Table 6.6.

For the Goodwin Avenue Basin the maximum allowable storage volume at manhole 51 is 35,000 ft^3. The results for unit storage costs of $0.50 and $0.10 per cubic ft, respectively, are given in Table 6.8.

6.5 Discussion of Examples

6.5.1 Examples Without Detention Storage

Table 6.5 makes three comparisons using the ASCE Basin. The left and center designs in the table show the effect of including the risk cost in the optimization. The installation cost is higher when risk is considered because larger diameter pipes are used to reduce the expected damage costs. However, if both risk and installation costs are considered a 16% total cost reduction is achieved by using the risk option.

The rational method design as presented in ASCE Manual 37 is shown on the right side of Table 6.5. Although the installation cost is slightly less than the design using the model without risk the comparison is misleading because three of the sewers are surcharged under design flows in the Manual 37 design. If these sewers were increased one size the installation cost would be about $45,600. In addition the expected damage cost is estimated because the risk analysis does not account for the surcharged situation.

A comparison using the Goodwin Avenue Basin is shown in Table 6.6. Again the effect of the risk option is seen. In this case a 39% reduction in total cost is achieved using the risk option. In this case the risk option design resulted in a substantial increase in the slopes of a number of the pipes over those for the design without risk. This was not as strongly seen for the ASCE Basin examples, possibly because of the elevation constraint at the outlet which was not present in the Goodwin Avenue examples.

6.5.2 Examples with Detention Storage

Tables 6.7 and 6.8 compare the results of the two detention storage options for the example basins. The general effect of storage is to permit the use of smaller pipes downstream of the reservoirs. The design of the upstream pipes

does not change.

In comparing the designs with no storage to those with non-optimized storage, for the ASCE Basin the pipe from manhole 81 to 82 was decreased from 36 to 27 in. and the slopes of the pipes downstream of the reservoir were reduced. For the Goodwin Avenue Basin all of the pipes downstream of the reservoir were reduced in size.

The designs using the storage optimization option illustrate the effect of unit storage cost. For lower unit cost the volume of storage and its cost is higher but this is more than offset by the reduction in installation cost. This is most easily seen for the Goodwin Avenue Basin where the storage cost increased from $137 to $3,035 while the installation cost was reduced almost $8000 resulting in a net cost reduction of almost $5000. For the ASCE Basin it is interesting to note that for $0.50 per cu. ft storage cost no storage was called for at manhole 83 while for the lower storage cost the model did call for storage there.

In all examples the storage optimization option resulted in lower total costs then without the option, as might be expected. However the comparison for the ASCE Basin shows very little cost reduction.

It should be pointed out that both storage options have their own advantage depending on the particular design criteria. If there is a limitation on flow then the non-optimization option could be used while a limitation on available storage volume may dictate the storage optimization option. If both flow and storage volume are limited both options could be used to find which constraint controlled.

6.5.3 Computer Requirements

There are currently two separate model programs. The first program contains all options except optimized detention storage. The storage requirement for this program is 30,608 words and the compilation time is 6.47 sec on the CDC Cyber 175 at the University of Illinois. The second program includes the detention storage optimization option and requires 33,409 words of storage and 7.17 sec to compile.

Table 6.9 shows a comparison of execution times for the various options for each example. Several conclusions can be made from this table.

(a) The additional time required for ILLUDAS generation of the inlet hydrographs is about 0.03 sec/pipe.

(b) The risk option increases the execution time by a factor of about 4, or an additional 0.6-0.8 sec/pipe.

(c) The non-optimization detention storage option requires essentially no additional execution time.

(d) The detention storage optimization option increases the execution time by a factor of 2-3 or an additional 0.3-0.5 sec/pipe.

TABLE 6.9 - Computer Execution Time

Basin	Risk	Storage (Non-Optimization)	Storage (Optimization)	Execution time in sec	
				Total	Time per pipe
ASCE	No	No	No	2.4	0.22
ASCE	Yes	No	No	10.5	0.95
ASCE	No	Yes	No	2.1	0.19
ASCE	No	Yes	Yes	8.9	0.81
Goodwin	No	No	No	3.1	0.22
Goodwin	Yes	No	No	12.4	0.88
Goodwin	No	Yes	No	3.1	0.22
Goodwin	No	No	Yes	7.6	0.54

CHAPTER 7 CONCLUSIONS AND RECOMMENDATIONS

7.1 Conclusions

This study has resulted in an improved design model with the following major features:

1. Design procedure based on a least-cost objective
2. Optional inlet hydrograph generation model for use at any specified inlet
3. Two detention storage options:
   a. A non-optimized detention storage option in which a maximum allowable downstream discharge is specified and the required storage volume is computed
   b. A detention storage volume optimization option in which the unit cost of storage is specified and the volumes corresponding to the least-cost design are computed
4. An improved risk damage cost option considering not only the probability of occurrence of damage but also the dependence of the damage on the flood volume
5. Flexible specification of pipe and excavation costs in tabular form
6. Capability of imposing specific constraints on elevations and size for any individual pipe

7.2 Recommendations

The following recommendations for improvements and increased capability are made:

1. Incorporate surcharge design capability as an option

2. Develop additional flexibility in cost specification
3. Develop a detailed user's manual which incorporates testing of actual design situations
4. Develop a flexible hydraulic description of detention reservoir operation to more closely approximate actual field operation
5. Develop the capability of design and/or analysis of hydraulic components such as pump stations and diversions
6. Modify the model so that combined sewer system design can be specified
7. Development of risk consideration when detention storage is considered
8. Develop nationwide cost functions for sewers, related structures, and damages

APPENDIX A

PROJECT PUBLICATIONS

The following publications were wholly or partially supported by projects C-4123 and B-098-ILL.

(1) Tang, W. H. and B. C. Yen, "Hydrologic and Hydraulic Design Under Uncertainties," Proceedings, International Symposium on Uncertainties in Hydrologic and Water Resource Systems, Vol. 2, pp. 868-882, Tucson, Arizona, Dec. 1972.

(2) Mays, L. W. and B. C. Yen, "Optimal Cost Design of Branched Sewer Systems," Water Resources Research, Vol. 11, No. 1, pp. 37-47, Feb. 1975.

(3) Yen, B. C., W. H. Tang, and L. W. Mays, "Designing Storm Sewers Using the Rational Method," Water and Sewage Works, Part I in Vol. 121, No. 10, pp. 92-95, Oct. 1974, Part II in Vol. 121, No. 11, pp. 84-85, Nov. 1974.

(4) Tang, W. H., L. W. Mays, and B. C. Yen, "Optimal Risk-Based Design of Storm Sewer Networks," Jour. Env. Eng. Div., ASCE, Vol. 101, No. EE3, pp. 381-398, June 1975.

(5) Mays, L. W., B. C. Yen, and W. H. Tang, "Worth of Data for Optimal Design of Storm Sewers," Proceedings, 16th Congress of the International Association for Hydraulic Research, Vol. 4, pp. 34-42, Sao Paulo, Brazil, July 1975.

(6) Yen, B. C. and A. S. Sevuk, "Design of Storm Sewer Networks," Jour. Env. Eng. Div., ASCE, Vol. 101, No. EE4, pp. 535-553, Aug. 1975.

(7) Yen, B. C. and W. H. Tang, "Risk-Safety Factor Relation for Storm Sewer Design," Jour. Env. Eng. Div., ASCE, Vol. 102, No. EE2, pp. 509-516, April 1976.

(8) Mays, L. W., "Optimal Layout and Design of Storm Sewer Systems," Ph.D. Thesis, Dept. of Civil Eng., University of Illinois at Urbana-Champaign, Illinois, 1976.

(9) Mays, L. W. and H. G. Wenzel, Jr., "A Serial DDDP Approach for Optimal Design of Multi-level Branching Storm Sewer Systems," Water Resources Research, Vol. 12, No. 5, October 1976.

(10) Yen, B. C., H. G. Wenzel, Jr., L. W. Mays and W.H. Tang, "New Models for Optimal Sewer Systems Design, " Environmental Modeling and Simulation, Proceedings of the U.S. EPA Conference, Cincinnati, Ohio, April 1976.

(11) Mays, L. W., H. G. Wenzel, Jr. and J. C. Liebman, "A Heuristic Model for Layout and Design of Sewer Systems," Jour. Water Resources Plan. and Manage., ASCE, Vol. 102, No. WR2, pp. 385-405, Nov. 1976.

(12) Yen, B. C., H. G. Wenzel Jr., L. W. Mays and W. H. Tang, "Advanced Methodologies for Design of Storm Sewer Systems," University of Illinois Water Resources Center Research Report No. 112, August 1976.

(13) Tang, W. H.; L. W. Mays; and H. G. Wenzel, "Discounted Flood Risks in Least-Cost Design of Storm Sewer Networks", Stochastic Processes in Water Resources Engineering, Proc. 2nd International IAHR Symposium on Stochastic Hydraulics, Lund, Sweden, Water Resources Publications, Fort Collins, Colorado, 1977, pp 293-317.